Solubility Measurements in the System CaSO₄–NaCl–H₂O at 35°, 50°, and 70° C and one atmosphere Pressure

by E-AN ZEN[1]

U.S. Geological Survey, Washington, D.C., U.S.A.

ABSTRACT

The solubilities in the system $CaSO_4$–$NaCl$–H_2O, at 1 atm pressure and 35°, 50°, and 70° C, have been determined by approaching the solubility curves from both the undersaturation and supersaturation sides. The experimental runs are of long duration, as much as 3 months; these rates should be commensurate with those of the appropriate geological processes, and so the results should be directly applicable to the interpretation of evaporite deposits.

Anhydrite was not precipitated from any solution composition in the ternary system. Instead, gypsum formed from solutions of all compositions at 35° and 50°, and from most solutions at 70°. In highly concentrated NaCl solutions and at 70° C, the hemihydrate (bassanite) forms. The isothermal, isobaric piercing points, in g/kg H_2O, are given below:

Phase	35°		50°		70°	
	CaSO₄	NaCl	CaSO₄	NaCl	CaSO₄	NaCl
Gypsum (G), Solution (L) . . .	2·30	0	2·16	0	2·05	0
Halite (H), L	0	362	0	365	0	376
G, H, L	7·0	360	6·6	363	—	—
Bassanite (B), G, L	—	—	—	—	8·4	278
H, B, L	—	—	—	—	6·4	375

A review of the existing thermodynamic data on the binary system $CaSO_4$–H_2O reveals that the data of Kelley *et al.* (1941) are not all internally consistent. If only consistent data are used, the calculated one-atmosphere transition temperature for gypsum and anhydrite in the binary system should be $46° \pm 25°$ C, instead of the 40° C frequently cited in the literature. The agreement between the calculations of Kelley *et al.* and experimental information, therefore, may be in part fortuitous. The experimental transition temperature, 41° C, may be too low because in nearly all earlier work the solubility curves were approached from the under-saturation side only; owing to the low angle of intersection of the gypsum and the anhydrite solubility curves, small errors in measurement would result in large changes in the transition temperature. The present values of gypsum solubility are about 5% higher than those reported in the literature.

The inability to synthesize anhydrite in the laboratory, in runs as long as 3 months, casts doubt on the efficacy of evaporative processes in precipitating anhydrite directly from sea water. Some anhydrite in the geologic record can be shown to be pseudomorphous after gypsum, but the origin of the bulk of the anhydrite is equivocal. If all sedimentary anhydrite resulted from dehydration of gypsum, however, the common occurrence of juxtaposition of bedded anhydrite and gypsum becomes puzzling. It is suggested that the composition of the entrapped connate water might serve as a memory device which could cause the dehydration process to occur on a bed-for-bed basis to result in the observed relations.

[1] Publication approved by the Director, U.S. Geological Survey.

INTRODUCTION

THE phase relations of the binary system $CaSO_4$-H_2O, in the range of stability of liquid water, have been studied by many investigators. This system is of geologic interest because it includes gypsum and anhydrite, two important minerals in evaporite beds; a third mineral in this system, bassanite, $CaSO_4 \cdot nH_2O$ ($n \leq \frac{1}{2}$), uncommon in nature, is used industrially as plaster of Paris. The binary system has been experimentally studied by Hall *et al.* (1926), Partridge & White (1929), Toriumi & Hara (1934), Hill (1937), Posnjak (1938), D'Ans *et al.* (1955), and Dickson *et al.* (1963), among others. Kelley *et al.* (1941) measured and compiled the thermochemical data on the solid phases in this system.

A geologically more useful system for study, however, is the ternary system $CaSO_4$-$NaCl$-H_2O because, in addition to the minerals listed above, it includes the important evaporite mineral halite,[1,2] with which gypsum and/or anhydrite is commonly associated. In fact, except for the carbonate phases that frequently accompany the evaporite minerals, phases in the ternary system closely model after the early products of evaporite deposition (Zen, 1962), and may be called a 'haplo-evaporite' system.

Experimental studies in the ternary system $NaCl$-$CaSO_4$-H_2O have been carried out by several people, for instance, Cameron (1901), Shternina (1947), D'Ans *et al.* (1955), Madgin & Swales (1956), Bock (1961), Blount & Dickson (1962), and Zen (1962). The anhydrite-gypsum relations in sea water have been investigated, though somewhat spottily; examples are the work of Toriumi *et al.* (1938), and Posnjak (1940).

Kelley *et al.* (1941) and Kelley (1960) measured and compiled thermodynamic data for the binary system $CaSO_4$-H_2O. Using the 1941 data, MacDonald (1953) calculated the effect of dissolved $NaCl$, as well as the effect of total and differential pressure, on the gypsum-anhydrite transition temperature. The data indicate that at one atmosphere total pressure the transition temperature in the binary system is 40° C; in saturated salt solution this temperature is lowered to 14° C. According to these data, at 35° C the transition from gypsum to anhydrite ought to occur in a solution of about 185 g $NaCl$/kg H_2O: in solutions of greater $NaCl$ concentration anhydrite alone could be stable. At 50° and 70° C, anhydrite alone should be stable at all $NaCl$ concentrations in the ternary system, up to the point of halite saturation. As will be seen, the experimental results contradict

---

[1] At very low temperatures, ice and a phase with the composition $NaCl.2H_2O$ are encountered, for instance, in the formation of sea ice in the polar regions (W. F. Weeks, Oct.-Nov. 1959, written communication). These phases, however, were not encountered in this work.

[2] The two components, $CaSO_4$ and $NaCl$, form a reciprocal system with $CaCl_2$ and Na_2SO_4. Available thermochemical data (Rossini *et al.*, 1952) show that at all temperatures dealt with in this work, the calcium sulfate and sodium chloride phases are more stable than the phases in the reciprocal system; furthermore, the phases dealt with in this work are all stoichiometric with respect to $CaSO_4$ and $NaCl$, so that the components $CaCl_2$ and Na_2SO_4 are never necessary in describing the system. In the present study, a few check runs have been made using $CaCl_2$ and Na_2SO_4 as starting materials. The results confirm the above assertion, as the product solid phases are gypsum and halite.

these thermodynamic predictions. The discrepancy is partly due to failure to attain stable equilibrium in the experimental runs, and partly due to uncertainties and imprecisions of the thermodynamic data used by MacDonald, whose calculations will be reviewed in a later section. The effect of pressure on the system $CaSO_4$–H_2O was also studied by Marsal (1952).

One significant feature common to most of the existing experimental studies, especially those in the 'low-temperature' range ($0°$–$100°$ C) is that the solubility values for gypsum, anhydrite, and bassanite were commonly derived from the direction of undersaturation alone. Thus, the solubility of a given phase in an aqueous solution is obtained by using an excess amount of the solid, and saturation is presumed when the amount of $CaSO_4$ dissolved apparently ceases to increase. At a given temperature, total pressure, and composition of the aqueous solution, the relative solubilities of gypsum and anhydrite, measured in this manner, are taken to indicate their relative instabilities.

This experimental approach is undoubtedly necessitated, in part, by the apparent impossibility of precipitating anhydrite from solutions, under conditions where anhydrite is presumed to be stable. Rather, if a solution is isothermally evaporated in the presumed stability field of anhydrite, gypsum or, under more restricted conditions, bassanite, separates out. Thus, it is not feasible to measure the solubility of anhydrite by reversible reactions.

The expedient of approaching the equilibrium curve from only one direction has its obvious dangers. For example, the rate of dissolution depends upon the crystallinity and grain size of the starting material in addition to the thermodynamic affinity (Prigogine & Defay, 1954, p. 52). If very fine grained but unsized material were used as starting material, the finer portion would dissolve first, leaving a high concentration of the coarse fraction; the rate of dissolution therefore would sharply decrease, a fact which might be erroneously interpreted as attainment of equilibrium. Moreover, in some studies, the criterion used for the attainment of saturation (for instance, the measurement of solution density by Madgin & Swales, 1956) may not be sensitive enough. Because the solubility curves of gypsum and anhydrite intersect at a low angle (see Posnjak, 1938), a relatively small error, say 10%, in the solubility determination would entail a large error in the transition temperature between these two phases.

For these and other reasons, it was felt that the low-temperature phase relations in the system $CaSO_4$–$NaCl$–H_2O were subject for further experimental study, with particular effort to approaching the solubility curve from both the undersaturation and the supersaturation sides. The results of this effort are presented in this paper.

EXPERIMENTAL

Details of starting material, equipment, and experimental procedure are given in Appendixes I–III. A brief summary suffices here.

Except for a few, early exploratory runs, all experiments were made with

natural gypsum and anhydrite to minimize the problem of possible side effects due
to the fine grain size of synthetic material. The starting materials are described
in Tables 1 and 2. Equilibrium (stable and metastable) was approached
both from the direction of supersaturation, using excess H_2O, and from the

TABLE 1

Starting material

Natural anhydrite: (1) Colorless, clear euhedral crystals, from Wathlingen, near Celle, Hanover, Germany (USNM R6004).
(2) Translucent, compact, colorless specimen, 'best' sample, Imperial Chemical Industries Mine, Billingham, Yorkshire, England.

Natural gypsum: (1) Selenite, Lockport, New York (USNM C4657).
(2) Selenite, Imperial Chemical Industries Mine, Billingham, Yorkshire, England.

Artificial gypsum: Baker reagent grade $CaSO_4.2H_2O$, batch P-322. Gypsum by X-ray diffraction.

Artificial anhydrite: Baker $CaSO_4.2H_2O$, above, ignited in muffle furnace at 300° C for 24 hours.

TABLE 2

Semiquantitative spectrographic data on the starting material, in percent[1]

Helen W. Worthing, analyst

	Anhydrite, Wathlingen	Anhydrite, Billingham	Gypsum, Billingham	Gypsum, Lockport
Si	0·0015	0·003	0·01	0·0007
Al	0·0015	0·0015	0·005	0·0007
Fe	< 0·003	< 0·003	0·003	< 0·003
Mg	0·007	0·0003	0·003	0·00015
Ca	Major	Major	Major	Major
Mn	0·0	0·00015	0·0	0·0
Ba	< 0·0003	< 0·0003	0·0005	< 0·0003
Cu	0·0015	0·00007	0·005	0·0003
Sr	0·3	0·3	0·02	0·003

Looked for but not found: Na, K, Ti, P, Ag, As, Au, B, Be, Bi, Cd, Ce, Co, Cr, Dy, Er, Eu, Ga, Gd, Ge, Hf, Hg, Ho, In, Ir, La, Li, Lu, Mo, Nb, Nd, Ni, Os, Pb, Pd, Pr, Pt, Rb, Re, Rh, Ru, Sb, Sc, Sn, Sm, Ta, Tb, Te, Th, Tl, Tm, U, V, W, Y, Yb, Zn, Zr.

[1] Results are reported in percent to the nearest number in the series 1, 0·7, 0·5, 0·3, 0·2, 0·15, and 0·1, and so forth; which represent approximate midpoints of group data on a geometric scale. The assigned group for semiquantitative results will include the quantitative value about 30% of the time.

direction of undersaturation, using excess solids. The latter approach, of course,
is the one used in most of the existing works on the system; solubility values thus
obtained are minimal values and the curves are, therefore, not necessarily the
true equilibrium curves.

The individual experiments lasted from between 10 days and 3 months,
depending on the temperature and the nature of the runs. Seeds of anhydrite
and/or gypsum were added to certain runs to induce crystallization. At the end
of each run, the solution was carefully filtered out, and weighed portions taken

for chemical analyses. The EDTA method was used for calcium determination, and a gravimetric method was adopted for total dissolved solids; from these data the weight proportions of the three components were readily computed.
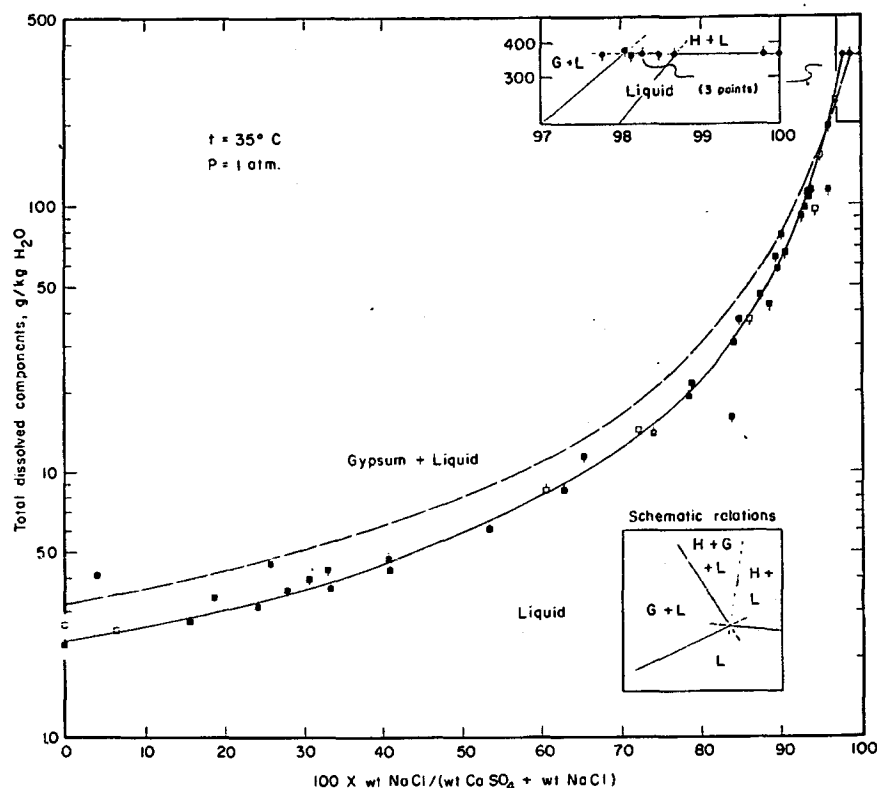

FIG. 1. Solubility relations in the system $CaSO_4$–$NaCl$–H_2O at 35° C and 1 atm pressure. The co-ordinates give compositions of the solutions. Symbols for product phases (Figs. 1–3): squares, gypsum; up-pointing triangles, anhydrite; down-pointing triangles, bassanite; circles, halite. Solid symbols if gypsum was the starting material; open symbols if anhydrite was the starting material. Leader above the symbol indicates that the run had excess solid (undersaturation runs); leader below the symbol indicates that the run was precipitative (supersaturation runs). The leaders thus indicate the direction in which the point should move if equilibrium were more nearly attained. Solid lines, observed solubility curves; long dashed line, the anhydrite solubility curve calculated from thermochemical data; short dashed lines, metastable extensions of solubility curves. The upper inset shows a portion of the solubility curves near the isobaric–isothermal piercing point on an exaggerated horizontal scale: the lower inset gives the schematic relations of the part of the diagram accessible to the liquid phase. The symbol '(3 points)' indicate triplicate runs.

The results are plotted and shown in Figs. 1–3 and also in Figs. 4–6 which include the data of D'Ans et al. (1955) and of Bock (1961) for comparison. The data are given in Tables 8–10.

The identification of solid phases at the end of each run depended primarily on immediate microscopic examination. The criteria used for halite were simply its cubic habit and optical isotropy. For those solutions high in NaCl concentration, some difficulty was encountered, because halite tended to precipitate

out of the solution on the slide, even with a slide cover in place. Crystal size was not a useful guide, as the 'secondary' halite could grow to large sizes in a few minutes. Experience showed, however, that primary halite crystals grown at temperature may be distinguished by the more clearly equant habit (the secondary crystals tend to grow as clusters of cubes, or into thin plates owing to the
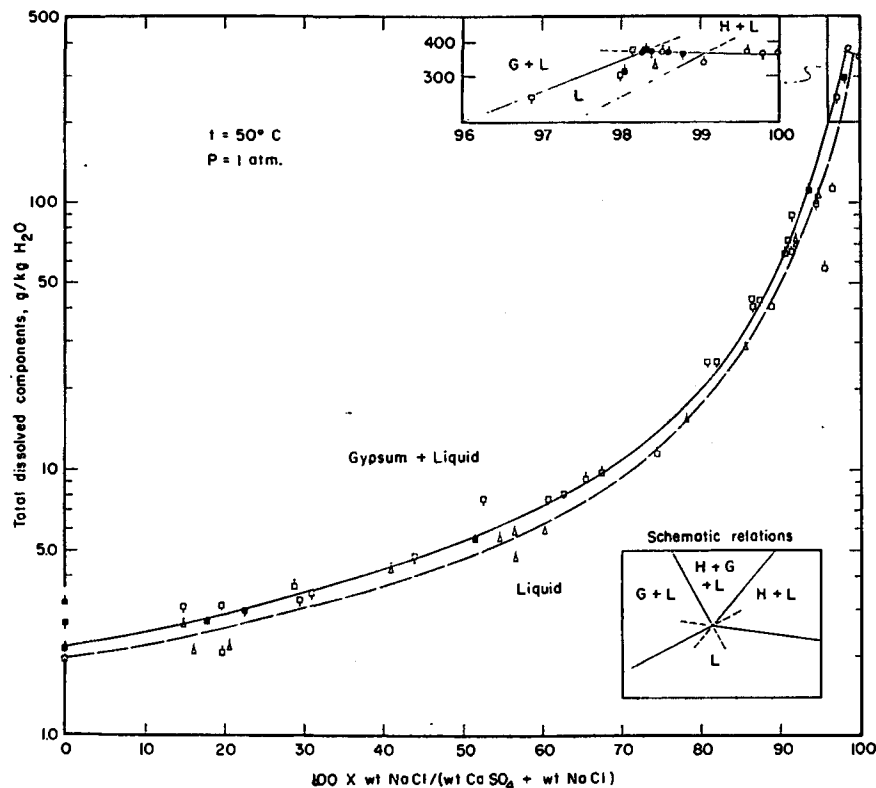

FIG. 2. Solubility relations in the system CaSO₄-NaCl-H₂O at 50° C and 1 atm pressure. See caption for Fig. 1 for explanation.

vertical confinement of the growth space), and by the trains of cubically oriented, tiny bubble inclusions which may have resulted in part from the hopper-type growth mechanism proposed by Dellwig (1955). These inclusions showed up, in plane polarized light, as zones of mottled grey colour. Finally, the primary halite crystals commonly showed unconformities of the bubble zones; this probably resulted from the crushing of the outer parts of the grains by the stirring magnets. Except where the amount of primary halite was minute, its presence was also readily detected in the flask by inspection.

Gypsum was readily identified by its monoclinic habit, its fish-tail twinning, and its non-parallel extinction. There has been no difficulty in distinguishing authigenic gypsum from 'detrital' gypsum which did not dissolve or which was

6233.1   K

added as seeds. The authigenic gypsum occurred as thin, delicate plates with large (010) faces, or as long needles (Fig. 7). Fish-tail or polysynthetic twinning was common, and the crystals were always euhedral. Because the crystal plates were thin, between crossed nicols they showed the first-order grey colour.
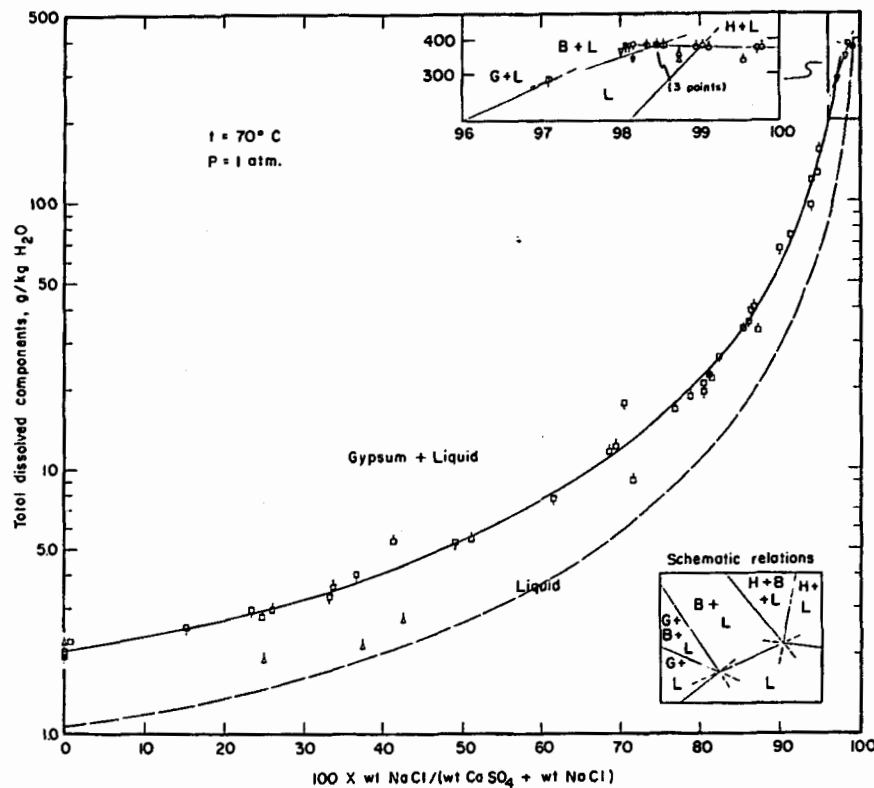

FIG. 3. Solubility relations in the system $CaSO_4$–NaCl–H_2O at 70° C and 1 atm pressure. See caption for Fig. 1 for explanation.

The detrital gypsum, on the other hand, occurred as stout, ragged laths, commonly with a pitted, dusty surface, and between crossed nicols generally showed higher order colours.

The seed anhydrite grains showed up as nearly equant fragments, commonly bounded by the three sets of cleavages (Fig. 7). These crystals showed vivid colours between crossed nicols and were commonly subrounded or showed corrosion re-entrants. Only 100×200 mesh anhydrite was used for seeds or in the 'excess solid' runs; the size of the material thus also aided in the recognition of detrital anhydrite.

No authigenic anhydrite has been noted in the runs except in run no. 145, made in a saturated solution of $CaCl_2$ at 70° C, given in Table 3. Under the microscope, the product material appeared as tiny, moderately birefringent
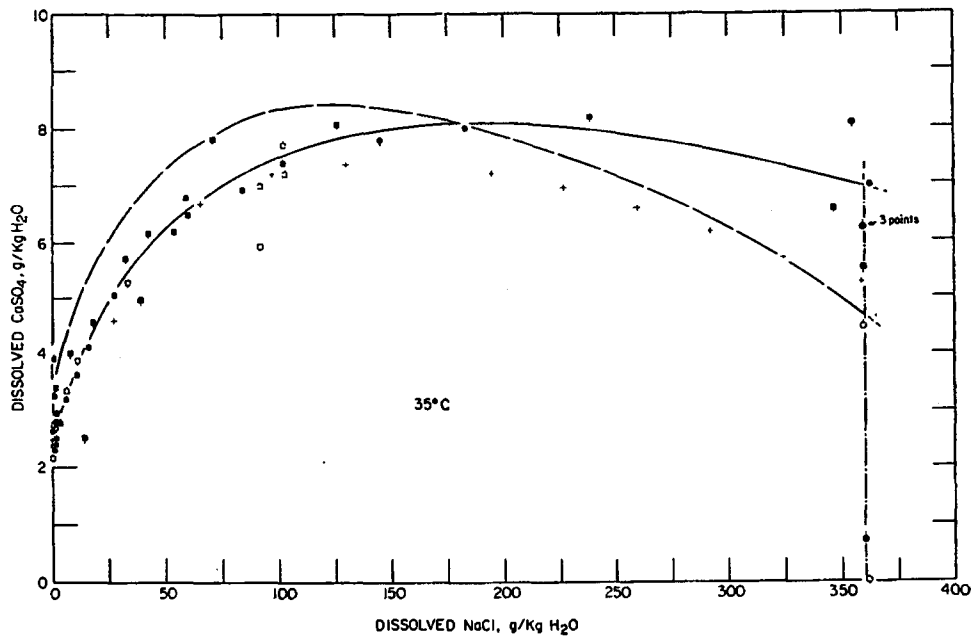
FIG. 4. Solubilities at 35° C in g NaCl and g CaSO₄ per kg H₂O. Symbols are same as those used in Figs. 1-3, with the following addition: +, the anhydrite solubility reported by D'Ans *et al.* (1955). Solid line, gypsum solubility curve; dash-dot line, halite solubility; long dashed line, calculated anhydrite solubility. Short dashes are metastable extensions.

FIG. 5. Solubility at 50° C. See caption for Fig. 4 for explanations. Additional symbols: *, gypsum solubility, and ⊗, anhydrite solubility, according to Bock (1961).

blebs; X-ray diffraction proved its identity as anhydrite. No good optical cri-
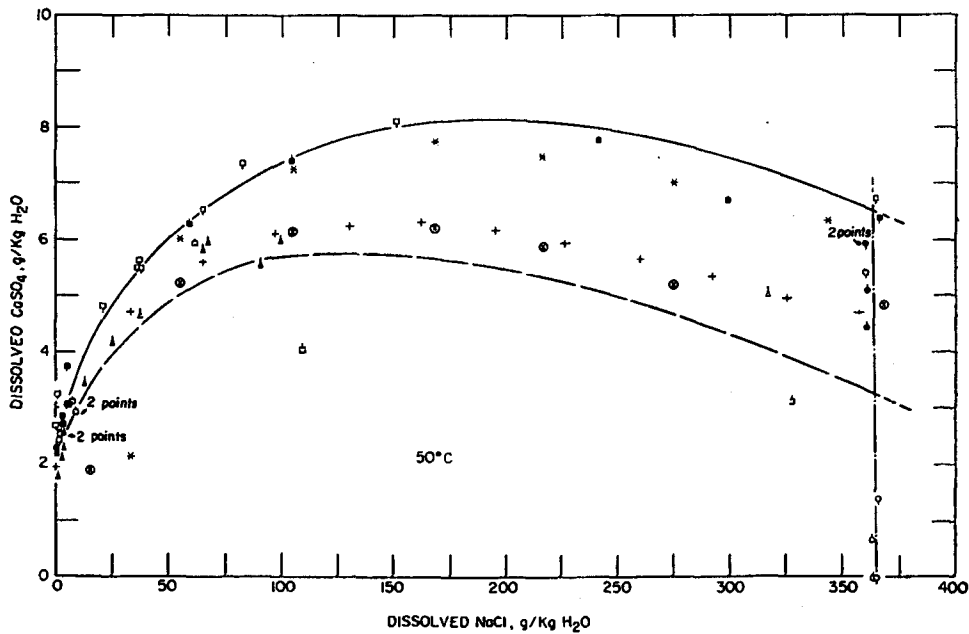terion for authigenic anhydrites was possible, unfortunately.

Bassanite was identified chiefly by its microscopic crystal habit; however,
the reliability of this guide was repeatedly verified by X-ray diffraction. The
crystals are stubby and spindle-shaped, showing moderate birefringence and
extinction parallel to the length (Fig. 8). The extinction is length-slow. The
width:length ratio seems to go up with crystal size, so that the smaller crystals
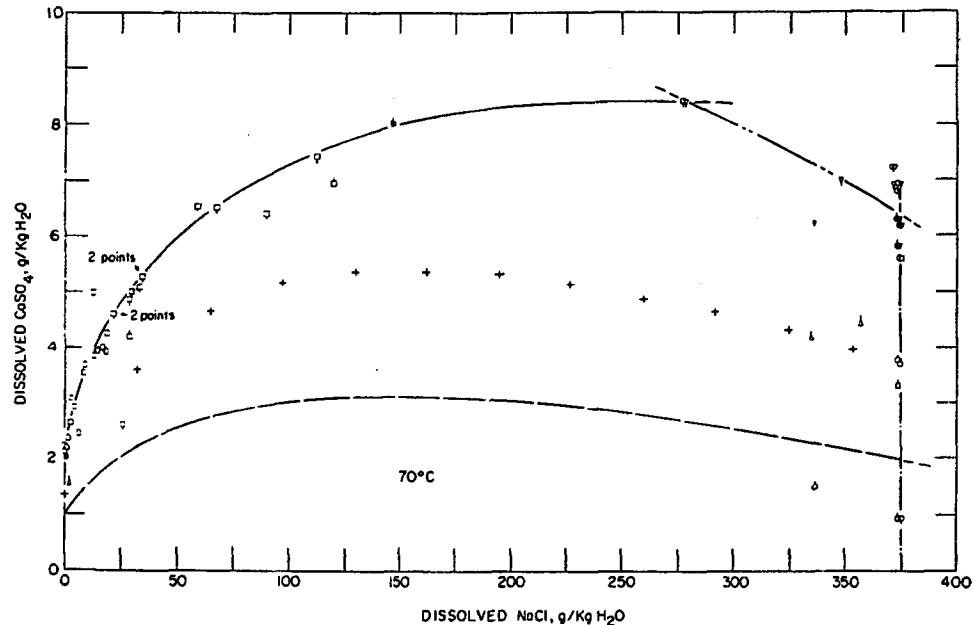

FIG. 6. Solubility at 70° C. See caption for Fig. 5 for explanations. Dash-dot-dot line, bassanite
solubility.

tend to be more acicular. Both between parallel and between crossed nicols, the
crystals show a peculiar greyish surface mottling whose origin is unknown but
which is characteristic of the phase and aids in its identification.

In the literature there is uncertainty as to whether calcium sulfate hemi-
hydrate ($CaSO_4 . \frac{1}{2}H_2O$) is a phase distinct from 'soluble anhydrite' ($CaSO_4$)
which may be prepared by carefully dehydrating the hemihydrate. Indeed,
Kelley et al. (1941, p. 15) mentioned two polymorphs of 'soluble anhydrite'
and two genetically related polymorphs of the hemihydrate. These phases (if
they be distinct) all have similar X-ray diffraction patterns (Weiser et al., 1936,
p. 1263; Posnjak, 1938, p. 253). The name bassanite applies to a mineral of the
same general X-ray diffraction pattern, but of unknown H_2O content (Palache
et al., 1951, p. 476).

Flörke (1952) analyzed the crystal structures of a hemihydrate and of a soluble
anhydrite. He concluded that the structures are basically the same, and that the
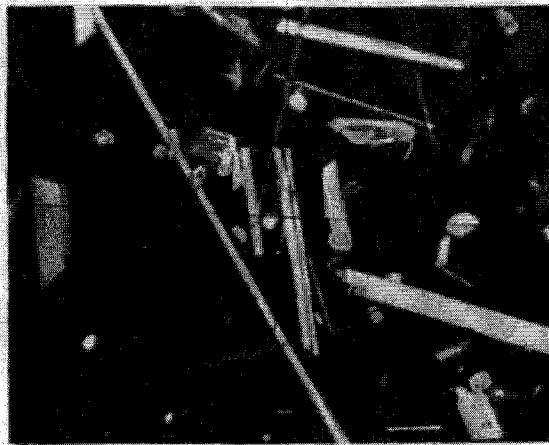
FIG. 7. Photomicrograph of gypsum (laths) precipitated from solution in the presence of anhydrite (subrounded, equant grains); run no. 174. Starting material: anhydrite and halite. 20 days at 50° C. Solution composition at end of run: 2·6 g CaSO$_4$ and 0·45 g NaCl per kg H$_2$O. Nicols crossed. The bar represents 0·1 mm.
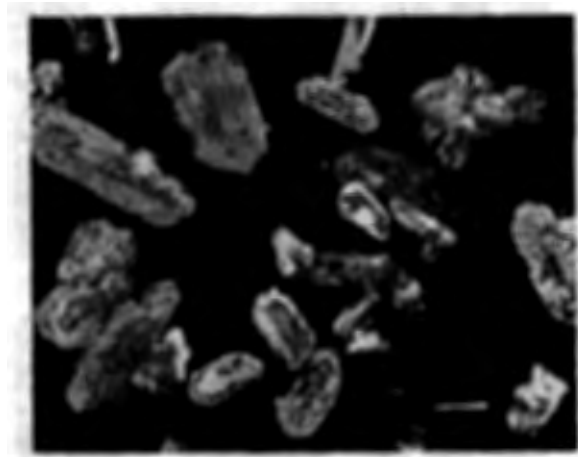
FIG. 8. Photomicrograph of bassanite from run 132. Starting material: gypsum and halite. 19 days at 70° C, with excess solid. Solution composition at end of run: 6·4 g CaSO$_4$; 374 g NaCl, per kg H$_2$O. Crossed nicols. The bar represents 0·1 mm.

differences in X-ray patterns are explicable in terms of distortions of the Ca and SO$_4$ positions by the introduction of H$_2$O molecules which are tied to the CaSO$_4$ framework by hydrogen bonds (pp. 211–14). These differences in X-ray patterns, therefore, are no proof that two phases are involved. The problem is recently summarized by Deer, Howie, & Zussman (1962, p. 206); its study is being continued in the laboratory. For the purpose of this paper, however, no phase distinction is attempted between the hemihydrate and the 'soluble anhydrite' phases; the name bassanite is used for the group whose optical properties and

X-ray pattern could fit either materials. Because in this work bassanite was encountered in such a restricted range of conditions, its composition and phase identity, whatever they are, are likely to be nearly constant. Because the temperature of crystallization of this bassanite was 70° C, it may be more nearly the hemihydrate, rather than the anhydrous, material.

The X-ray patterns of the solid phases were compared with standard patterns; for bassanite, the pattern of commercial plaster of Paris has been used; this agrees with the data of the A.S.T.M. file and those of previous workers. The patterns of all four solid phases are clear cut and distinct; it is estimated that

TABLE 3

Data on anhydrite synthesis

Starting material:	Natural gypsum (Billingham), excess.
	c.p. CaCl₂, excess.
	water, 150 ml.
Temperature:	70° C.
Type of run:	Excess solid.
Length of run:	22 days.
Density of solution:	about 1·4 g/ml.
Weight % CaCl₂:	About 40%.
Solid produced:	Microscopically indeterminable owing to the opacity of the solution. anhydrite+gypsum in the 'water insoluble' fraction. X-ray diffraction: anhydrite+subsidiary gypsum.

the X-ray method can detect a phase if it is more than 5% of the bulk. In practice, the strongest and diagnostic lines are used for phase identification. These are the 11·8° line of gypsum, the 13·5° line of bassanite, the 25·5° line of anhydrite, and the 31·8° line of halite (CuKα radiation).

The need to examine the solids immediately at the end of each run cannot be overstressed. For example, in prolonged runs at such temperatures and solution salinities that anhydrite should be stable, this phase commonly converted to gypsum, albeit incompletely. The measured $CaSO_4$ solubility in such a system presumably reflects the solubility of gypsum and not of anhydrite, so that the presence of a solid phase in excess is no guarantee that its solubility is being measured, as is assumed in some previous work. If the secondary gypsum is in small amounts, it might not be detected by X-ray diffraction of the product; however, undelayed optical examination, preferably of several slide mounts, should indicate its presence. The conversion of anhydrite to gypsum under conditions where anhydrite is presumed to be stable is one of the surprises of this study and will be considered again.

As a second example of the possible pitfalls in phase identification by X-ray diffraction, prompt optical examination of the solid product of one run showed bassanite and halite, plus seed crystals of anhydrite. The moist sample was not rinsed with acetone but was left to dry in open air. When X-rayed a few days later, the dominant pattern was that of gypsum, with only ancillary bassanite!

Microscopic examination of this material confirmed gypsum to be dominant; bassanite was relict and corroded (Fig. 9). Apparently, despite the high salinity of the solution, at room temperature the process of hydration of bassanite was
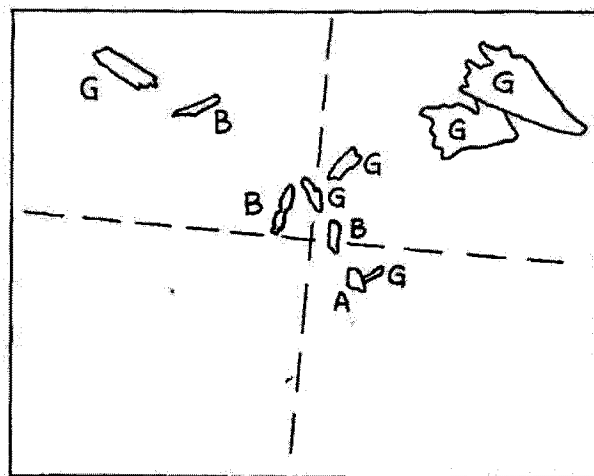
FIG. 9. Photomicrographs of bassanite, gypsum, and seed anhydrite. The identities of the individual grains are shown in the accompanying sketch. Run no. 178. Starting material: anhydrite and halite. 13 days at 70° C. Solution composition at end of run: 6·9 g CaSO₄ and 372 g NaCl per kg H₂O. Immediate examination of the run product under the microscope showed only anhydrite and bassanite; the gypsum was converted from bassanite at a later stage. Nicols crossed.

able to proceed nearly to completion. If the X-ray technique alone were used, the nature of the solid products could have been grossly mistaken.

In general, microscopic examination of the solids was made within 2 minutes of removal from the flask at temperature; commonly the time lapse was shorter. The X-ray runs could wait for days if the solids were separated from the mother

liquor and rinsed with acetone. Because NaCl is insoluble in acetone, this rinsing process causes the NaCl in the water solution to precipitate out in a flash. The precipitate occurred as milky white curds which could be washed out with little difficulty.

DISCUSSION OF THE RESULTS

Graphical representation of the data

In terms of weight units, the solubility of halite is some 150 times that of gypsum and anhydrite at the same temperature. The quantity, dissolved $(CaSO_4 + NaCl)$, in gm per kg H_2O, is therefore conveniently represented on a logarithmic scale, and is plotted against the weight percentage of NaCl in the dissolved material, on a linear scale. Despite this choice of co-ordinates, however, clearly all the *local* properties of phase diagrams, such as the Morey–Schreinemakers Rule (see, for instance, Morey & Williamson, 1918, pp. 65–66), must be obeyed as usual. The diagrams (Figs. 1–3) exaggerate the experimental scatter in the low-solubility region but de-emphasizes the scatter in the high-solubility region. The experimental data are also plotted in terms of grams of dissolved NaCl and $CaSO_4$ per kg H_2O (Figs. 4–6).

Invariant points

The three isothermal sections in Figs. 1–3 were studied at one atmosphere pressure. For each isothermal section, thus, a binary 'invariant' point (actually a piercing point) has two condensed phases, and a ternary 'invariant' (actually piercing) point has three condensed phases.

The bounding binary piercing points studied involve halite and its saturated solution, or involve gypsum and its saturated solution. According to the thermodynamic data of Kelley *et al.* (1941), at 50° and 70° C the stable binary invariant point in the $CaSO_4$–H_2O system should involve anhydrite and its saturated solution. As mentioned previously, however, the solubility curve of anhydrite could not be determined reversibly because, despite the use of coarsely crystalline anhydrite as the starting material and the use of anhydrite seeds, this phase could not be precipitated from solution. The (metastable?) binary piercing point involving gypsum and solution, on the other hand, is readily studied and could be reversed reproducibly.

The binary points for gypsum and solution have the compositions of 2·30, 2·16, and 2·05 g $CaSO_4$ per kg H_2O, at 35°, 50°, and 70° C, respectively. This is to be compared with the values of 2·1, 2·08, and 1·95 g per kg H_2O, which represent data compiled by Posnjak (1938, p. 268). The present figures are 4–9% higher than the literature results. Posnjak (1938, p. 264) pointed out that too high solubility values would result, and did result in some earlier work, if fine-grained material were used, and if extra care were not used in filtering the solution to exclude all suspended solids. Neither of these causes could be responsible for the present high values. The best explanation seems to be that the literature data were obtained from approaching the solubility curve from the

undersaturation side only, but the present data are the averages of measurements with equilibrium approached from both directions.

The binary solubility of halite in water is given as 361, 368, and 375 g/kg H_2O (6·18, 6·29, and 6·41 molal), at 35°, 50°, and 70° C, respectively (*International Critical Tables*, v. **4**, p. 235). These values are to be compared with the present values of 362, 365, and 376 g/kg H_2O. The agreement is good, especially in view of the fact that the *International Critical Tables* values are not individual determinations, but represent smoothed values from composite measurements.

TABLE 4

Compositions of isothermal, isobaric piercing points, in g per kg H_2O

Phase	35°		50°		70°	
	CaSO₄	NaCl	CaSO₄	NaCl	CaSO₄	NaCl
Gypsum (G), Solution (L)	2·30	0	2·16*	0	2·05*	0
Halite (H), L	0	362	0	365	0	376†
G, H, L	7·0*	360*	6·6*	363*	—	—
Bassanite (B), G, L	—	—	—	—	8·4*	278*
H, B, L	—	—	—	—	6·4*	375*
Anhydrite (A), L	3·14*	0	1·92	0	1·05	0
A, G, L	8·0	180	—	—	—	—
A, H, L	4·8	360	3·3	364	2·0	375

* Metastable point.   † Extrapolated.

The ternary piercing points at both 35° and 50° C involve gypsum, halite, and solution; available data indicate that these are metastable piercing points because the stable point is concerned with anhydrite instead of gypsum. The experimental determination of these ternary points is more difficult than of the binary points. From the undersaturation side, the piercing point was located simply by using excess anhydrite and halite as starting material; at the end of the run the solids consisted of gypsum and recrystallized halite (plus relict anhydrite), all in a mat at the bottom of the flask. Analysis of the solution gave the liquid composition at the piercing point. The location of the point was confirmed by the compositions of solutions in gypsum (and anhydrite)-free or halite-free systems on the two sides of the piercing point.

The location of a ternary piercing point from the supersaturation side is less precise, for it is difficult to hit upon the correct $CaSO_4$: NaCl ratio in advance. In practice, then, this point was approached by allowing first one solid to precipitate, and the second one to join it upon continued evaporation. Owing to nucleation difficulties, the equilibrium piercing point could be easily overshot; the problem was alleviated by reaching the apparent ternary point along both the gypsum and the halite solubility curves. The true location of the piercing point was taken as intermediate within the range of apparent ternary points, and between the line thus defined and the apparent location of the point from the undersaturation side. The compositions of the ternary piercing points, thus determined, are given in Table 4. The uncertainty, assessed on a weight

NaCl-weight $CaSO_4$ plot (Figs. 4–6), is ± 5 g NaCl and ± 0.2 g $CaSO_4$ (per kg H_2O); this is about 1.5% in NaCl and 2% in $CaSO_4$.

At 70° C, two ternary piercing points were observed, neither, however, with great precision. The points involve gypsum–bassanite-solution, and bassanite-halite-solution; the compositions are given in Table 4. The lack of precision was caused in part by the difficulties in quenching the NaCl-rich solution, in part by the problem of identifying small amounts of bassanite (which could be confused with tiny fragments of relict anhydrite), and in part, at least, by the close proximity of the two piercing points. The problem of pinning down each point thus became amplified. Indeed, some runs yielded gypsum and halite, suggesting that the metastable points involving bassanite might be metastably suppressed with ease.

Univariant lines

A ternary system that consists of two phases is truly trivariant; if temperature and pressure are held constant, however, it is univariant and will be so referred to in this paper.

At 35° C there are two univariant lines, representing saturation with gypsum and halite; parts of both lines, in the neighbourhood of the ternary piercing point, are presumably metastable. At 50° C the same lines are determined, but the entire gypsum saturation curve, as well as part of the halite curve near the piercing point, are presumably metastable. At 70° C three univariant lines are observed, representing saturation with gypsum, bassanite, and halite. The former two and part of the last curve are presumably metastable. As noted previously, it may even be experimentally feasible to suppress the bassanite univariant curve altogether.

For all three isotherms, the halite solubility curve is believed to be fairly reliable. This situation is due to (1) the ease of crystallization of halite, so that the solubility curve is readily measured reversibly and with close tolerance; and (2) the fact that at this composition range, small errors in $CaSO_4$ chemical analysis affected the computed solubility curve but little. It will be noted that the halite solubility curve, or its metastable extension, includes the entire set of stable or metastable piercing points that involve halite, liquid, and one of the solid phases that contain $CaSO_4$. Among the points of this set, those which are relatively the more stable lie closer to the NaCl–H_2O binary boundary, and vice versa. These relations will be used in another context.

The location of the bassanite solubility curve at 70° C is fixed only by the location of the two terminating piercing points, gypsum–bassanite-liquid and bassanite–halite-liquid. Because the two points are close together, the location of the univariant curve is reliable to the same extent that the locations of the piercing points are known.

The solubility curves for gypsum involve large composition ranges and sharp changes in curvature (which would be even more pronounced than shown in

Figs. 1-3 had a linear plot been employed). These curves were arrived at by plotting the experimental points both as shown in the projection of Figs. 1-3, and in the projection of Figs. 4-6. The curves were adjusted and smoothed on both projections until a satisfactory agreement was obtained. One guideline used was that no reversal in the curvature was allowed. Such a reversal seems improbable on theoretical grounds, as a matter of fact it was not required by the empirical data.

At 35° and 50° C the solubility of gypsum per kg H_2O increases with NaCl content in solution to a maximum, then decreases slightly before reaching the piercing point. The location of this maximum point is not precise, but is around 180 g NaCl and 8·05 g $CaSO_4$ per kg H_2O at 50° C; and 225 g NaCl and 8·1 g $CaSO_4$ per kg H_2O at 35° C. The 'salting-out' effect has also been noted by Shternina (1957) and by Magdin & Swales (1956).

At 70° C no 'salting-out' was observed for gypsum. The rate of increase of gypsum solubility with increasing NaCl content decreases, however, to approach zero, until the experimental curve was terminated by the metastable gypsum-bassanite-solution piercing point. This feature suggests that the solubility maximum would be found on the metastable extension of the univariant curve. Indeed, the solubility of bassanite decreases with increasing NaCl between the two piercing points (Table 4).

Calculation of the anhydrite solubility curves

As the reversible determination of the anhydrite solubility curves in the ternary system could not be made, their positions must be calculated from the gypsum curves with the aid of existing thermochemical data on these phases. Because over much of the range of interest the concentration of salts in the solution phase is so high that no theory of electrolytic solution applies, the calculation must be approximate and *ad hoc* to an extent. Several approaches have been combined; the calculations for the 35° C isotherm will be used to illustrate the method.

For the $CaSO_4$-H_2O binary, the solubility of anhydrite is computed by means of the Debye–Hückel theory. Because the solubility of gypsum, 2·3 g/kg H_2O, corresponds to an ionic strength of only about 0·07, the Debye–Hückel theory, especially in the extended form of Robinson & Stokes (1955, p. 230), certainly ought to apply:

$$\log \gamma_{\pm} = \frac{-A|Z_1 Z_2| I^{\frac{1}{2}}}{1+Ba_i I^{\frac{1}{2}}} + bI \qquad (1)$$

where $\gamma_{\pm}$ is the mean activity coefficient, I the ionic strength, A, B, and a_i constants of the Debye–Hückel theory, Z_1 and Z_2 the ionic charges, and b the constant of Robinson and Stokes. The values of A and B are taken from Klotz (1950) and are shown in Table 5. For a_i, an 'average' value of 5×10^8, applicable to the entire ternary system, was used. The value for b in the binary system is 0·4 (Robinson & Stokes, 1955, p. 230).

Using these constants and the observed solubility of gypsum, $\gamma\pm$ for gypsum saturation (designated γ^G hereafter) is readily computed. To extend the result to anhydrite, it is necessary to make use of the thermochemical data in the literature.

Kelley *et al.* (1941) gave $\Delta G°$ for the reaction

$$\text{Gypsum} = \text{Anhydrite} + 2 \text{ water (liquid)} \qquad (2)$$
$$\text{CaSO}_4 \cdot 2\text{H}_2\text{O} \qquad \text{CaSO}_4 \qquad 2\text{H}_2\text{O}$$
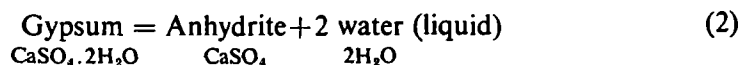
as a function of temperature, at 1 atm total pressure. The equation is now modified and brought up to date (see next section) to bring about greater consistency of the data; the result is

$$\Delta G° \ (T, 1 \text{ atm}) = -2{,}890 + 179 \cdot 40 \ T + 0 \cdot 026 \ T^2 - 30 \cdot 98 \ T \ln T \qquad (3)$$

in calories. At 35° C, $\Delta G° = +137$ cal for reaction (1) to the right.

TABLE 5

Debye–Hückel constants used in the computations

Temperature, °C	A	$B \times 10^{-8}$	$a_i \times 10^{+8}$	Reference
35	0·5175	0·3297	5	Klotz, 1950, p. 330.
50	0·5319	0·3321	5	Same.
70	0·5533*	0·3355*	5	

* Graphically extrapolated from Klotz's data for 0°–60° C.

At gypsum saturation, we can write

$$G^G \ (T, 1 \text{ atm}) = \mu_{\text{CaSO}_4} \text{ (gyp sat)} + 2\mu_{\text{H}_2\text{O}} \text{ (gyp sat)}$$

where μ is the chemical potential. Similarly, at anhydrite saturation

$$G^A \ (T, 1 \text{ atm}) = \mu_{\text{CaSO}_4} \text{ (anh sat)}.$$

At a given temperature, therefore,

$$G^G - G^A = \mu_{\text{CaSO}_4} \text{ (gyp sat)} - \mu_{\text{CaSO}_4} \text{ (anh sat)} + 2\mu_{\text{H}_2\text{O}} \text{ (gyp sat)}$$

and we also have

$$\mu_{\text{CaSO}_4} \text{ (gyp sat)} - \mu_{\text{CaSO}_4} \text{ (anh sat)} = RT \ln a^G/a^A$$

where the activities a refer to CaSO_4 in solutions saturated with respect to the indicated phases, and an unspecified, common reference state is used for both a^A and a^G. Therefore,

$$\ln \frac{a^G}{a^A} = \ln\left(\frac{\gamma^G n^G}{\gamma^A n^A}\right) = \frac{1}{RT}\left[-\Delta G° + \int_{N=1}^{N'} \left(\frac{\partial \mu_{\overline{\text{H}}_2\text{O}}}{\partial N_{\text{H}_2\text{O}}}\right)_{T,P} dN_{\text{H}_2\text{O}}\right] \approx \frac{-\Delta G°}{RT} \qquad (4)$$

where n is the molal concentration of CaSO_4 in the saturated solution, $\Delta G°$ is exactly the quantity in (3), and N is the mole fraction of H_2O in the solution; N' corresponds to a gypsum-saturated solution at the particular temperature

and pressure. The approximation shown involves a free-energy difference of only about 2 cal and is adopted for all the subsequent calculations.

The quantity, $\ln \gamma^A n^A$ ($= \ln a^A$), can be evaluated from equation (3), the experimental data, and the results of calculations using the Debye–Hückel theory. The value for n^A is next obtained by successive approximation, as follows. First we set $\gamma^A = \gamma^G$; this leads to a value of n^A from which the value of I, the ionic strength, can be calculated. Using (1), a new value of γ^A is obtained, which leads to a refinement of n^A, and so on. The iteration is continued until the resulting n^A is constant to a value corresponding to 0·01 g/kg H₂O. The anhydrite solubility thus obtained is 3·14 g/kg H₂O for the binary, 35° C isotherm.

It is possible to extend the technique into the ternary system, because within the range of validity of the Debye–Hückel theory, a given NaCl concentration (in g per kg H₂O), contributes to the ionic strength by a constant amount which can be calculated. The constant b in (1), however, is no longer 0·4 because a uni-univalent component has been added. Robinson and Stokes (1955, p. 230) suggest that $b = 0·1\ Z_1 Z_2$, so that $b \approx 0·2$ at a NaCl mole fraction of 0·8 in the ternary system. Interpolated values must be used for intermediate compositions. Fortunately, the error introduced by an incorrect assignment of b is small. At a NaCl mole fraction of 0·8, the ionic strength is about 0·17, which may exceed the range of validity of the Robinson and Stokes formula; however, for the present purpose the formula is assumed to remain approximately valid.

The iteration procedure is precisely the same as that used for the binary system; this is so because at a given temperature the product $\gamma^A n^A$ must be a constant value, corresponding to anhydrite saturation, irrespective of the presence of NaCl in the solution. In the ternary system, however, starting out with a given NaCl fraction on the gypsum solubility curve, the calculations lead to a different NaCl fraction as well as a different value for the total dissolved salt, on the anhydrite curve.

The portion of the anhydrite curve in the high NaCl range may be computed only with much less precision. The procedure used is as follows. The NaCl content, in g per kg H₂O, is noted for a number of points on the gypsum solubility curve. Using the H₂O vapor pressure data for the system NaCl–H₂O (*International Critical Tables*, v. 3, p. 370), the quantity $\Delta\mu_{H_2O}$ for the appropriate isotherm, as a function of the dissolved NaCl content, is computed by the formula

$$\Delta\mu_{H_2O} = RT \ln p/p_0$$

where p_0 is the vapor pressure of H₂O over pure H₂O water and p the vapor pressure of H₂O over a given solution.

The value of free energy change for the gypsum–anhydrite reaction for the given NaCl content is then[1]

$$\Delta G^* = \Delta G^\circ + 2\ \Delta\mu_{H_2O}.$$

[1] An error is introduced at NaCl mole fraction $\approx$ 0·8 or less because then the contribution of CaSO₄ to $\Delta\mu_{H_2O}$ becomes comparable to that of NaCl. However, in this range $\Delta\mu_{H_2O}$ is itself a very small quantity, and the correction would not be noticeable.

The value of γ^G is simply obtained by the relation

$$\gamma^G = \gamma^G(O)\ n^G(O)/n^G$$

where the notation (O) refers to the values in the NaCl-free binary system. For the quantity γ^A, the iterative method proves to be impractical because the series fails to converge satisfactorily. γ^A is approximately obtained, however, by plotting the ratio γ^A/γ^G within the range of validity of the Debye–Hückel theory and
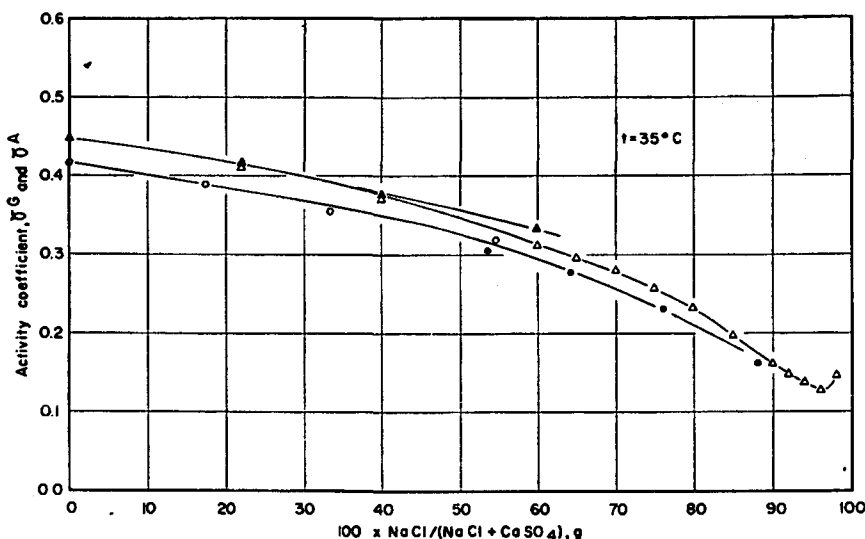
FIG. 10. Activity coefficients of $CaSO_4$ in the ternary system $CaSO_4$–$NaCl$–H_2O at 35° C. Solid triangles, activity coefficients in gypsum-saturated solutions (γ^G), calculated using the Robinson–Stokes extension of the Debye–Hückel formula; open triangles, γ^G calculated from the observed $CaSO_4$ solubilities in the ternary system; open circles, activity coefficients in anhydrite-saturated solutions (γ^A), calculated using the Robinson–Stokes extension of the Debye–Hückel formula and the 'consistent' thermochemical data for the system $CaSO_4$–H_2O; solid circles, γ^A calculated by extrapolating the γ^A/γ^G ratio derived from the Debye–Hückel formula, as explained in the text. The reversal of slope at the high NaCl end indicates the 'salting-out' effect on gypsum in NaCl-rich solutions.

extrapolating to the more concentrated solutions. Knowledge of a given set of values for n^G, γ^A, and ΔG^* then gives a point on the anhydrite solubility curve.

The values of γ^G and γ^A derived by the several methods are plotted against the fraction of NaCl; these are shown in Figs. 10–12 for the three isotherms. As can be seen, in all cases it is possible to draw a single smooth curve through the two sets of values of γ^G. At 50° and 70° C, $1 > \gamma^A > \gamma^G$, reflecting the assumed fact that anhydrite is more stable than gypsum. At 50° C, $\gamma^G \approx \gamma^A$ because this temperature is close to the binary transition temperature; at high NaCl concentrations, the values for γ^G and γ^A should diverge because the transition temperature is lowered by the NaCl; however, this effect is swamped, because the ionic strength of the solution is dominated by the contribution from NaCl.
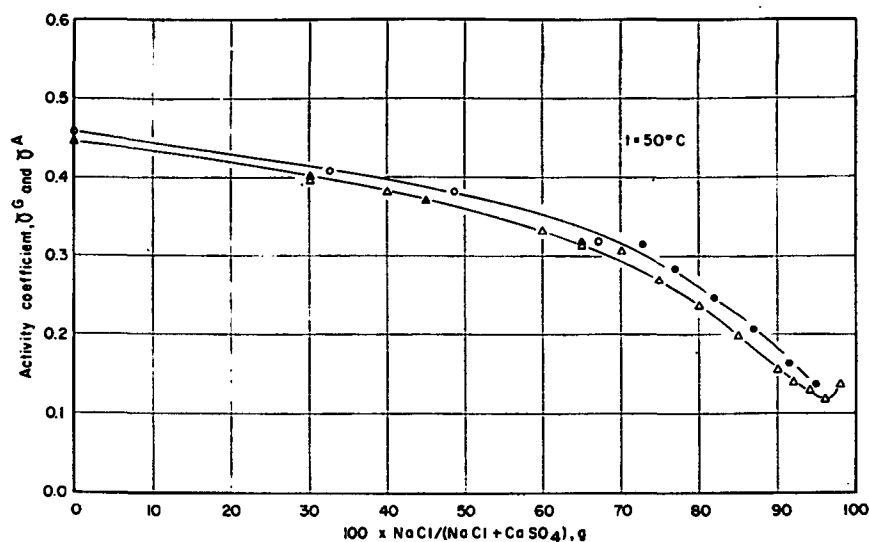
Fig. 11. Activity coefficients of $CaSO_4$ in the ternary system $CaSO_4$–$NaCl$–H_2O at 50° C. See caption for Fig. 10 for explanation.
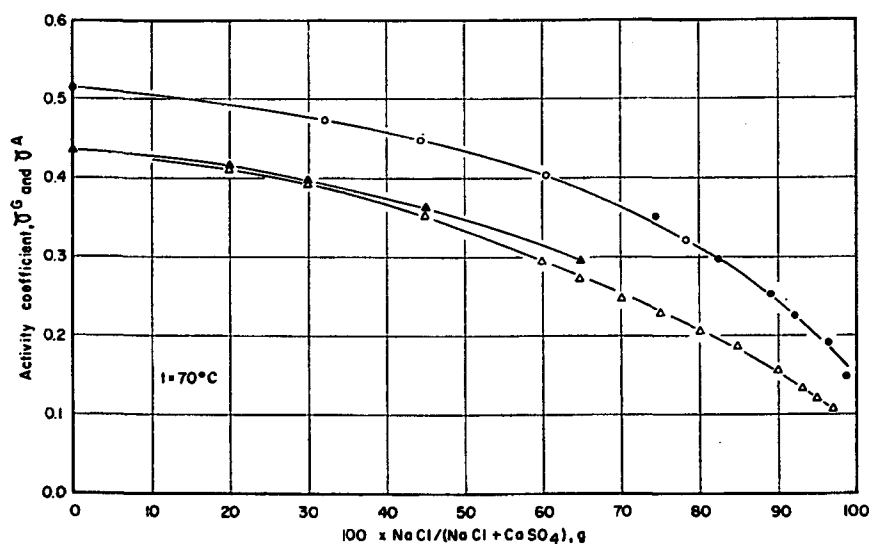
Fig. 12. Activity coefficients of $CaSO_4$ in the ternary system $CaSO_4$–$NaCl$–H_2O at 70° C. See caption for Fig. 10 for explanation.

Computation of the anhydrite curve at 70° C made use only of the gypsum-solubility curve; the bassanite curve is very limited in extent, so that its use is not necessary.

At 35° C the values of γ^A, based on the Debye–Hückel theory, lie below those of γ^G, because within this range of data anhydrite is more soluble. The two curves should cross at about 96 weight per cent NaCl (see Fig. 1).

The computed invariant points that include anhydrite are included in Table 4.

The anhydrite–gypsum transition relation in the ternary system, here reported, cannot be compared with previous calculations, for instance by MacDonald (1953), because the thermochemical data used are slightly different. To an examination of these data we next turn; matters caloric to learn and spurn.

A re-examination of the thermochemical data

The thermochemical data used by MacDonald (1953) to calculate the gypsum–anhydrite transition in sea water (which he approximated by NaCl solutions) are those of Kelley *et al.* (1941, p. 44). These workers gave for the reaction

$$\text{Gypsum} = \text{Anhydrite} + 2 \text{ water,}$$

$$\Delta G^\circ = -2495 + 163 \cdot 89 \; T + 0 \cdot 0215 \; T^2 - 28 \cdot 30 \; T \ln T \qquad (5)$$

which leads to a transition temperature of 313° K or 40° C, in agreement with the experimental data of Posnjak *et al.*

The function ΔG° (T) of Kelley *et al.* is not internally consistent. In obtaining the expression, the authors (1941, p. 43) used $I = -33 \cdot 18$ for an integration constant. This is the mean of their own, consistent calorimetric value of $-33 \cdot 03$, and an independent value of $-33 \cdot 34$, reported by Toriumi and Hara (1934) from indirect vapor-pressure measurements. Differentiating (5), we get, at 25° C,

$$-\partial \, \Delta G^\circ / \partial T = \Delta S^\circ = 12 \cdot 83 \text{ cal/mole/deg.}$$

Using the probable entropy values for the phases, given in Table 6, this leads to S° for water (pure H_2O) of 16·8 e.u., instead of the accepted value of $16 \cdot 75 \pm 0 \cdot 03$ e.u. (Giauque & Stout, 1936).

A revised value for the heat capacity of anhydrite is now available (Kelley, 1960, p. 46). Using this new value, and also the 'consistent' value of $I = -33 \cdot 03$, integration leads to the expression, already cited,

$$\Delta G^\circ \; (T, \; 1 \text{ atm}) = -2,890 + 179 \cdot 40 \; T + 0 \cdot 026 \; T^2 - 30 \cdot 98 \; T \ln T \qquad (3)$$

which gives ΔS (25° C) as 12·6 e.u., and the correct value of S° for 100%-H_2O water of 16·75 e.u.

Equation (3) predicts that the gypsum–anhydrite transition temperature in the binary system should be 46° C instead of the 40° C cited in the literature. There is thus a discrepancy between 'consistent' thermochemical data and published experimental results.[1] However, the published solubility curves of Posnjak (1938, p. 268) and of Kelley *et al.* (1941, p. 55) are consistent also with a transition temperature of 46° C. Posnjak's anhydrite curve shows experimental points on both sides of the curve; however, because all these data points

---

[1] It should be noted that, in constructing the stability diagram for the system $CaSO_4$-H_2O, Kelley *et al.* (1941, p. 55) constrained the gypsum and anhydrite curves to intersect at 40°, citing the thermodynamic data, and remarking that the empirical solubility values are scattered in the low-temperature range (p. 56).

pertain to approach to equilibrium from the undersaturated side, the true curve should lie above the points; such a shift would raise the transition temperature to about 45° C.[1]

The uncertainties in the thermodynamic data for gypsum and for anhydrite should be noted. The heat of hydration value for the gypsum–anhydrite reaction in the binary system is uncertain by ± 20 cal according to Kelley *et al.* (1941, p. 15); to this should be added 14 cal/mole of H_2O from discrepancies in

TABLE 6

Entropy data at 25° C

Phase	Formula	Entropy cal/mole/deg K	Reference
Anhydrite	$CaSO_4$	$25 \cdot 5 \pm 0 \cdot 4$	Kelley *et al.*, 1941, p. 19.
Gypsum	$CaSO_4.2H_2O$	$46 \cdot 4 \pm 0 \cdot 4$	Ibid.
'Bassanite'	$CaSO_4.\frac{1}{2}H_2O^*$	$31 \cdot 8 \pm 0 \cdot 6$	Ibid.
'Bassanite'; $= \alpha$-soluble anhydrite	$CaSO_4$	$25 \cdot 9 \pm 0 \cdot 3$	Ibid., p. 23.
'Bassanite'; $= \beta$-soluble anhydrite	$CaSO_4$	$25 \cdot 9 \pm 0 \cdot 3$	Ibid.
'Bassanite'; $= \alpha$-hemihydrate .	$CaSO_4.\frac{1}{2}H_2O$	$31 \cdot 2 \pm 0 \cdot 6$	Ibid., p. 24.
'Bassanite'; $= \beta$-hemihydrate .	$CaSO_4.\frac{1}{2}H_2O$	$32 \cdot 1 \pm 0 \cdot 6$	Ibid.
Water	H_2O	$16 \cdot 75 \pm 0 \cdot 03$	Giauque & Stout, 1936.

* Consisted of 75% α and 25% β forms of the hemihydrate.

the heat, free energy, and entropy of vaporization of water. The uncertainty in ΔS, as given in Table 6, is $\pm 0 \cdot 86$ e.u.; for $\Delta G°$ therefore we have

$$\partial \Delta G° = 48 \pm 0 \cdot 86 \ T. \tag{6}$$

These data are shown in Fig. 13, where the heavy solid line depicts $\Delta G°$ according to equation (3), and the heavy dashed line, $\Delta G°$ according to equation (5). The light lines give the uncertainties according to (6). The existing thermochemical data do not fix the gypsum–anhydrite transition temperature to better than $\pm 25°$ C about either 40° C or 46° C.

Additional thermochemical calculations are given in Appendixes IV and V.

[1] Posnjak has no experimental datum between 37° and 47·5° C for anhydrite, and none between 38° and 50° for gypsum (1938, p. 267). Data for these cited temperatures were derived from runs of a few days' duration which probably were insufficient for equilibration. If the anhydrite solubility were but 5 per cent too low (corresponding to an error of 0·01 weight per cent), the transition temperature would be low by about 5° owing to the flat intersection of the gypsum and anhydrite solubility curves. In this connexion, it is interesting to note Bock's (1961, p. 1748) results on the gypsum–anhydrite transition temperature as a function of the NaCl content of the solution. Bock's data extrapolate smoothly to a transition temperature of 47° C at zero NaCl content; in order to fit the 41° temperature reported in the literature, he had to give the univariant curve an abrupt bend. Bock's results are suspect, however, because the runs were of short durations (2 or 4 days), excess solids were used for all the runs, and the starting material was c.p. reagent gypsum and its ignited, anhydrous product, rather than natural, coarsely crystalline material. Apparently the resulting solid phases were not identified. Thermodynamic values calculated from Bock's data show non-random errors of appreciable magnitude.

GEOLOGIC IMPLICATIONS AND APPLICATIONS

General remarks

The phase–equilibrium study of the system $CaSO_4$–$NaCl$–H_2O was among the first laboratory work of this sort to be applied to natural rock bodies. One of the earliest scientific studies of the system was by Lavoisier (1768). Discussion of the geologic applications are legion since the works of Van't Hoff (1912);
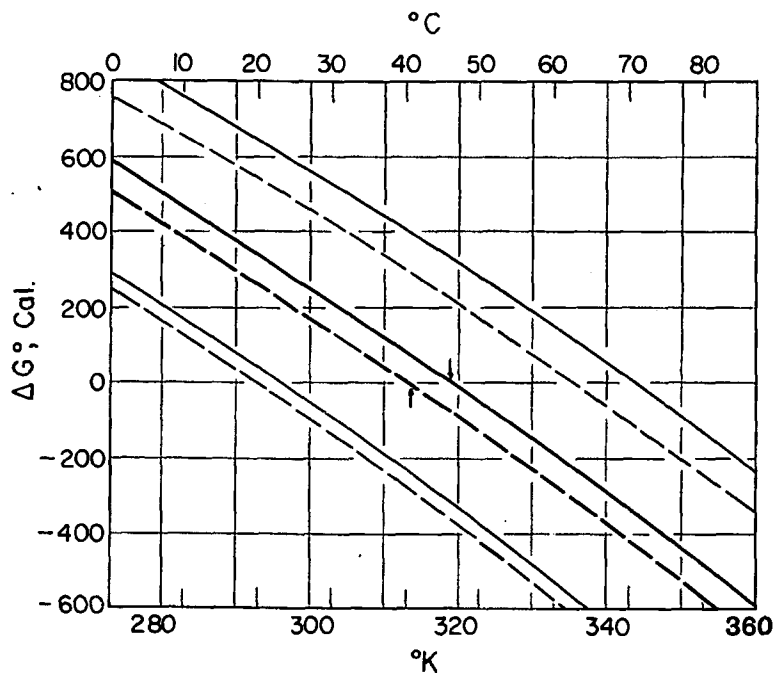
FIG. 13. Gibbs free energy change for the reaction gypsum = anhydrite+2 water, at 1 atmosphere pressure. Heavy solid line, using 'consistent' data according to equation (3); heavy dashed line, using the data of Kelley *et al.*, equation (5). The light solid and light dashed lines give the thermochemical uncertainties according to equation (6) for the two situations, respectively.

one of the most recent being that of MacDonald (1953). Borchert (1959), Stewart (1963), and Braitsch (1962*a*) recently summarized our knowledge. It is not necessary to repeat the discussions here, and only selected topics will be considered.

Origin of sedimentary anhydrite beds

The geologic records show many evaporite stratigraphic sections in which gypsum beds are succeeded upward by anhydrite beds, or in which these two types of beds alternate in a vertically (and therefore temporally) persistent fashion (see, for example, Udden, 1924; Schaller & Henderson, 1932; Adams, 1944; Raymond, 1953; Stewart, 1963; Braitsch, 1962*b*). Because a gypsum bed commonly passes upward into an anhydrite bed, which in turn passes upward

into a halite bed, the sequence corresponds to the result of continued desiccation of sea water. Many anhydrite beds of evaporite sequences therefore have been taken to be the result of direct precipitation (for instance, MacDonald, 1953; Dellwig, 1955, p. 105; Briggs, 1958). On the other hand, there has been persistent doubt among some workers that all or the bulk of the evaporite anhydrite beds could be primary (for instance, Posnjak, 1940, p. 567; Borchert & Baier, 1953; Conley & Bundy, 1958; D'Ans & Kühn, 1960). This doubt resulted in part from the inability of workers to synthesize anhydrite under geologically reasonable conditions of temperature and pressure, and in part from the petrographic observations, for instance by Stewart (1953) that, in the Permian anhydrite deposits of Yorkshire, England, many anhydrite crystals are aggregates that exhibit gross outlines characteristic of twinned gypsum. It is clear that at least some anhydrite deposits are 'metamorphic', and were transformed from gypsum. This evidence, however, cannot be extrapolated; it does not prove either that the anhydrite was deposited as gypsum, or, contrariwise, that no gypsum was deposited as anhydrite.

The present experimental results shed light on the problem of natural anhydrite deposits, for two reasons. First, the experimental runs were of long duration. Although natural anhydrite beds of great aggregate thicknesses no doubt were accumulated over long periods of time, individual layers of crystals probably were laid down in periods measured in months or less. It is unlikely that temperatures of deposition could have been higher than 50° C, so that the conditions of the present experimental work should be applicable with little or no extrapolation.

Secondly, the present work attempted to approach the solubility curves from the 'precipitation' side as well as from the 'solution' side, and so constitutes realistic approximations to the natural processes. With the looming problem of metastable equilibria, certainly in the artificial and likely in the natural systems as well, the need to specify the process is imperative. The fact that the presence of anhydrite seeds did not affect the precipitating phase is also pertinent in this context.

For these reasons, it seems plausible that many, if not most, sedimentary, bedded anhydrite deposits in evaporite sections must have originated as gypsum beds; these beds later, perhaps after burial, mildly metamorphosed to become anhydrite beds. W. T. Holser (1962, unpublished memorandum) studied the literature for criteria to distinguish anhydrite derived from primary precipitation and from later alteration. It seems that no unambiguous rule is possible; one might question the validity of the criterion of crystal habit. On the other hand, anhydrite crystal aggregates which are pseudomorphs after fish-tailed crystals (Stewart, 1953) may be taken as proof that the anhydrite is after gypsum, which itself may or may not be primary in origin. The great majority of the sedimentary anhydrite deposits, however, give no indication whatever of their original mineralogy which must remain an open question.

Perhaps one of the stoutest arguments that may be marshalled against the presumption of secondary origin for anhydrite beds is this: a given evaporite section commonly contains both beds of gypsum and beds of anhydrite. These beds may be in close spatial association. If the anhydrite were originally gypsum, why did the process of phase transformation that occurred subsequent to deposition not affect all the beds alike? Why should the post-burial, probably polymetamorphic conversion preserve the bedded nature of the deposits? And finally, why should the lithic sequence, namely beds of gypsum–anhydrite–halite, be present in accordance with the theoretical model for chemical equilibrium during deposition?

A possible answer, albeit speculative, is that the connate fluid entrapped within and around the primary crystals at the time of deposition might have served as 'memory' devices. Roedder (1963) studied the nature of fluid inclusions in crystals of various geologic origins, and showed that the composition of the fluids may be faithful records of the nature of the mother liquor during the precipitation of the crystal. Thus, if two gypsum beds were deposited at the same temperature and pressure, but one of these was formed from a solution significantly more saline than the other, the differences in the chemical micro-environments for the two beds might be preserved in inclusions and as inter-stitial water if no significant cross-formational circulation had occurred. If these beds, upon burial, were converted to anhydrite, then later reconverted in a near-surface environment, the bed with a less concentrated bathing solution would have a greater tendency to be converted to gypsum, everything else being equal.

Another possible explanation for the discrepancy between experimental results and the field relations of gypsum–anhydrite interbedding is that the ternary system may not be a good approximation of sea water. Although NaCl is the dominant dissolved component in sea water, other components, notably $MgSO_4$, are important. Whether these components suffice to influence the precipitation relations of gypsum and anhydrite, either through nucleation effects or through further depression of the chemical activity of H_2O, is uncertain. Conley & Bundy (1958) found that, at 40° C, the addition of K_2SO_4 to the system $CaSO_4$–H_2O resulted eventually in the intermediate phase syngenite, $CaK_2(SO_4)_2H_2O$, rather than in the conversion of gypsum to anhydrite; however, this result is directly in conflict with those of Hill (1937), who reported reversible measurements of anhydrite solubility in the same ternary system at 35° and 45° C. This contradiction is unresolved.

Origin of massive and of banded monomineralic evaporite beds

A major problem encountered in the interpretation of evaporite deposits is the origin of thick and areally extensive beds which are monomineralic and which may be tens of feet thick. A vast amount of sea water must be dehy-drated to produce each bed; the problem is especially acute for the sulfate beds

because of the low content of $CaSO_4$ in sea water. Replenishment of sea water is obviously necessary, yet the replenishment must take place so as not to disturb the prevailing physicochemical equilibria between the residual water and its precipitate, at least so as not to leave a record of the disturbance in the sedimentary column.

The unlikelihood of such delicate balance, over wide areas and long periods, under the scheme of conventional bar-basin hypothesis of evaporite deposition, has caused considerable restudy of the problem. Significant contributions were made by Borchert (1959, and references cited therein), Braitsch (1962*b*), Scruton (1953), and Briggs (1958), among others. Borchert & Tollert (see Borchert, 1959) proposed a 'dynamic polythermal' model in which temperature differences are allowed in different parts of the evaporating water body. Depending on the relative values of the temperature coefficients of solubility, the various precipitated phases could become segregated in different parts of the basin, resulting in sharp, lateral changes of the mineral assemblages (Borchert, 1959, p. 39). Moreover, Borchert's experiments also showed that the existence of thermal gradients induced the metastable extension of the crystallization fields of various phases (p. 34). Borchert's observations, however, were strictly empirical; no theory of electrolyte solution exists yet which allows the prediction of the temperature coefficients of solubility of phases in a multicomponent system on the basis of measurements in the simpler subsystems.

The mechanism proposed by Briggs (1958) invokes the idea of 'influx equilibrium' and fractional crystallization in a current that flows into a basin of evaporation; this steady-state model does not postulate temperature differences. Briggs pointed out (p. 49) that the thickness as well as nature of the evaporite is a clue to the original current pattern; using these criteria he derived an elegant reconstruction of the paleogeography of the Salina evaporite basins of Michigan, New York, and Ohio. Briggs's mechanism is in many respects akin to that of Scruton (1953).

An open-system, steady-state model was proposed by Zen (1959, 1960) to account for monomineralic evaporite deposits. As in Briggs's model, it invokes fractional crystallization and attainment of only local equilibrium; but temperature and pressure differences are allowed and their petrographic consequences accounted for. Indeed, Zen used temperature differences as the chief means to cause succession of different monomineralic beds.

Isothermally and isobarically, entire ranges of solutions should be able to precipitate a given phase, for instance gypsum; this could account for the areal extensiveness of the evaporite beds. Thermal gradients obviously might either extend or abbreviate the range. Within wide ranges, changes in solution composition would not be reflected in the compositions of the solid phases, which, at least within the ternary system $CaSO_4$–$NaCl$–H_2O, are all stoichiometric. As suggested in an earlier section, however, fluid inclusions and interstitial water, trapped at the time of deposition, might have different compositions;

these differences conceivably could trigger the reconversion of some anhydrite beds into gypsum upon surface exposure, while leaving other beds unaltered. Such a mechanism, if valid, would result in bedded gypsum–anhydrite–halite sequences.

The steady-state model was used by Zen (1960) to explain the banded, monomineralic and rhythmic salt deposits. The fact that the layers are individually monomineralic precludes their deposition in a system where the chemical potentials of the components are internally buffered ('initial value components', Zen, 1963); rather, these components must be of the 'boundary value' type. A bar basin, with either occasional replenishment, or with periodic changes in the composition of the surficial water layer as proposed by Braitsch (1962*b*), should result in cycles of precipitation in which the components belong to the 'initial value' category, even though the system is open, as any evaporating system must be. In general, a bar-basin model could have rhythmic, banded beds, but only the first layer of each cycle could be monomineralic. The sequence would be gypsum–gypsum and halite, or gypsum–anhydrite–anhydrite and halite; instead of the commonly observed gypsum (or anhydrite)–halite. It appears, therefore, that the various modifications of the bar-basin theory cannot be reconciled with theories of phase equilibrium, if the petrographic observations of monomineralic beds or at least laminae are indeed correct.

ACKNOWLEDGEMENTS

APPENDIX I

STARTING MATERIAL

The experiments used only natural gypsum and anhydrite, except as otherwise stated. The samples are described in Tables 1 and 2; they were all free of phase impurities. The samples were ground and two size fractions were used: between 100 and 200 mesh, and −200 mesh. The former was used exclusively for approaching equilibrium from the undersaturation side in order to reduce the likelihood that the solubility might be affected by grain size. The −200-mesh fraction was used for approaching equilibrium from the supersaturation side in order to hasten the reaction.

The halite was Baker Reagent Grade NaCl, used without further refinement.

Early in the study, Reagent Grade $CaSO_4.2H_2O$ was tested as starting material. The sample consisted of fine-grained (about 20 microns), euhedral gypsum crystals

that gave a good X-ray pattern. Dehydration of this material at 300° C in a furnace overnight produced fine aggregates of anhydrite with a clear, sharp, X-ray pattern and free of any trace of other phases. However, when brought into contact with water, this anhydrite readily reverted to gypsum; such artificial anhydrite therefore is unusable as starting material for long-duration runs. Because the natural material is chemically quite pure, it has been used in the majority of the runs.

APPENDIX II

EXPERIMENTAL PROCEDURE

All the runs were made in 500-ml Pyrex Erlenmeyer flasks using distilled water. Samples of the solid starting material were weighed out; in general from 0·5 to 2 gm of $CaSO_4$, and up to 80 gm of halite, were used for the gypsum–anhydrite portions of the solubility curves. The 'excess solid' runs contained 200 ml H_2O, and the 'excess H_2O' runs contained 400 ml H_2O to ensure the presence of enough solution for chemical analyses when subsequent evaporation had caused sufficient solids to precipitate out for study. For an 'excess H_2O' run, the flask was opened after the solids had dissolved; an aluminum foil was lightly fitted around the mouth of the flask to allow slow evaporation and to prevent contamination. Commonly, at the end of the evaporation process, the flask was stoppered for a few days to allow the annealing of the phases before they were sampled.

Several water baths of different construction and degrees of temperature control were used. For the 70° isotherm, only baths with mercury regulators were used and the temperature controls are believed to be good to 0·2° C. For the 35° and 50° isotherms, baths with bimetallic strip controls were also used; the temperatures were good to at least 0·5° C because the bath water was in all instances constantly stirred and all the baths have large thermal inertia. The thermometers used in all the baths were calibrated against a −1° to 101° C, mercury-in-glass thermometer, graduated to 0·1° C, that had been certified by the National Bureau of Standards.

The solutions were stirred, mechanically through sealed couplings, or magnetically. Some runs were stirred only occasionally by mechanical shaking.

The duration of each run depended on the nature of the run and on the temperature. At 70° C runs of 10 days commonly sufficed to ensure saturation or precipitation. The 50° C isotherm is based on runs generally of 3 weeks or longer, and the 35° C isotherm is on runs of 2 months or longer. At these lower temperatures, evaporation of the 'excess H_2O' runs was especially tardy because the air surrounding the bath was nearly saturated with H_2O, and runs as long as 3 months were often necessary. These lengths may be comparable with those corresponding to natural evaporite deposition.

Pyrex crucibles with fritted filter disks were used to sample the solutions. These crucibles were extended with extra lengths of glass tubing for convenience. Upon the completion of each run, the crucible assembly, pre-heated to temperature, was lowered into the solution and gentle suction was applied through a vacuum system. The first portion of the filtrate was discarded. Three consecutive portions of the solution were then pipetted out, each from a fresh filtrate. One portion of the solution, between 5 and 10 ml, was drained rapidly into a weighing bottle; two portions, between 2 and 5 ml. depending on the Ca concentrations, were drained into weighed polyethylene bottles fitted with screw caps. After as much of the solution was filtered out as

practicable, a sample of the solid phases was immediately transferred on to a glass slide and examined under the petrographic microscope. The bulk of the solid was then transferred out of the flask, thoroughly rinsed with acetone to remove the interstitial solution, and X-rayed after drying. In most instances, so little solution remained after the filtration process (barely enough to keep the solids moist) that little secondary reaction was likely within the short time during which the sample, out of the bath, was removed from the flasks.

After recording its weight, the solution in the weighing bottle was slowly evaporated to dryness in an oven at 45° C. The residue, loosely covered, was then heated to 400° C overnight in a muffle furnace. Tests showed that the final heating temperature sufficed to convert all the $CaSO_4$ phases to anhydrite and to destroy fluid inclusions, yet did not cause the halite to volatilize. Care was taken to check for possible loss of solids by decrepitation; none was observed. The solid, in the weighing bottle, was weighed to constant weight over a period of several days, and the weight of dissolved ($NaCl+CaSO_4$) per 1,000 gm solution was computed. The precision is $\pm 0.5\%$.

The weights of the duplicate solution samples in polyethylene bottles were recorded and the samples were analyzed for calcium by the EDTA methods. The analyses were made by personnel of the U.S. Geological Survey under the supervision of W. W. Brannock and Leonard Shapiro; the method has been described by Brannock and Shapiro (1962). The duplicate samples were analyzed on different occasions by different technicians to avoid any systematic bias. The results generally agree to $\pm 5\%$. From the calcium analysis and the gravimetric analysis for total dissolved salts, the weight proportions of $CaSO_4$, $NaCl$, and H_2O in each solution are readily computed.

The extraction of liquid, by using a slight vacuum over the filter crucible, no doubt led to some vaporization of H_2O. The magnitude of this error is unknown, but the error would result in too great solubility values. However, because the upper end of the extended crucible assembly was above the top of the Pyrex flask, and at a lower temperature, there was invariably condensation from the vapor and part of this condensate refluxed into the solution. The two factors, therefore, tended to compensate each other. In practice, both effects were minimized by keeping the extraction train vertical and the inflow of liquid even. By extending the tip of the sampling pipette to the lower part of the filtrate, only 'fresh' solution was sampled. The refluxed water, being less dense, did not tend to mix freely with the bulk of the solution.

APPENDIX III

SEEDING

For most of the early runs, and all of the later experiments, all the 'excess H_2O' runs were seeded, either by starting the evaporation cycle before all the solids had dissolved, or by adding seeds to the clear solution. Because gypsum precipitates readily, even in the absence of seeds, under conditions which ought to result in anhydrite, the seed crystals always included anhydrite (100×200 mesh), although some runs were charged with a mixture of anhydrite and gypsum seeds.

It was reasoned that, in the 'excess H_2O' runs, small, invisible nuclei of the starting material might have persisted, to influence the nature of the precipitated phase, even when the solutions were optically clear. For runs in regions where anhydrite should be the stable phase, therefore, as a rule anhydrite was used as the starting material. This

precaution apparently made no difference in the identity of the product phase. Conceivably, the metastable formation of gypsum, especially in the runs with open flasks, could have been caused by thin surface films of cool and/or supersaturated solutions which were not equilibrated with the bulk of the system. The constant stirring of the contents of the flasks should have effectively eliminated this possibility. As a further check, the local temperatures of the contents of several flasks were measured with a chromel-p-alumel thermocouple. The results of the measurements are given in Table 7.

TABLE 7

Local temperatures in flasks

Test	Bath temperature	Location of thermocouple	mv	Temperature difference, °C
1	70° C, flask not stirred	Bottom of flask	set = 0	
		Half-way up liquid column (about 2 cm)	−0·01	−0·25
		Just below liquid surface	−0·06	−1·5
		1 mm above liquid surface	−0·17	−4·25
2	70° C, stirred magnetically	Bottom of flask	set = 0	
		Just below liquid surface	−0·01	−0·25
		Just above liquid surface	−0·11	−2·75
		In air column 5 cm below mouth of flask	−0·13	−3·25
3	50° C, not stirred	Bottom of flask	set = 0	
		Just below liquid surface	−0·02	−0·50
		Just above liquid surface	−0·15	−3·75
		In air column 5 cm below mouth of flask	−0·35	−8·75
4	35° C, not stirred	Bottom of flask	set = 0	
		Just below liquid surface	−0·03	−0·75
		2 mm above liquid surface	−0·05	−1·25
		In air column 2·5 cm below mouth of flask	−0·17	−4·25

From this it is clear that, without stirring, a temperature difference of up to 1·5° C could exist in the liquid column; with stirring, however, the gradient was absent. Certainly, the discrepancy between the predicted limiting equilibrium temperature of gypsum formation, and the observed temperature where it formed, generally greatly exceeded the temperature difference in the flasks. This explanation of local cold spots, therefore, is inadequate.

APPENDIX IV

REVISION OF THERMODYNAMIC CALCULATIONS

MacDonald's calculations on the gypsum–anhydrite equilibrium (1953) was based on the data of Kelley *et al.* (1941), which have been discussed previously. As was shown, when only self-consistent data are employed in the thermochemical calculations, the equilibrium temperature for the gypsum–anhydrite transition is 46° C instead of 40° C. In addition to the value of the intercept on the temperature axis, the

TABLE 8

Experimental data on the system $CaSO_4$–$NaCl$–H_2O. I. 35° C Isotherm at 1 atm pressure

Run no.	Length, days	Seeds	Starting material*	Approach†	Solution results, g/kg H_2O where applies				Solid phases‡
					$CaSO_4$	NaCl	($CaSO_4$+NaCl)	$\dfrac{CaSO_4}{(CaSO_4+NaCl)}$	
17	29	A, G	A (cp)	S	2·41	0	2·41	1·00	G
29	23	G, A	A (W)	U	2·20	0	2·20	1·00	G
35	23	—	A (cp)	U	2·79	0	2·79	1·00	G
36	23	—	G (cp)	U	2·28	0	2·28	1·00	G
37	34	no	G (cp)	S	2·67	0	2·67	1·00	G
43	19	no	A (cp)	S	2·64	0	2·64	1·00	G
45	21	no	G (cp), H	S	5·76	31·76	37·52	0·154	G
46	15	—	G (cp), H	U	3·21	5·42	8·63	0·372	G
47	31	no	G (cp), H	S	4·60	17·40	22·00	0·209	G
56	42	—	G (cp), H	U	2·81	3·23	6·04	0·465	G
57	38	no	G (cp), H	S	4·05	7·58	11·63	0·348	G
62	32	—	G (cp), H	U	3·97	0·17	4·14	0·959	G
83	36	—	G (cp), H	U	2·43	1·20	3·64	0·668	G
84	43	no	G (cp), H	S	3·41	1·19	4·60	0·741	G
85	36	—	G (cp), H	U	3·30	0·72	3·02	0·761	G
90	107	no	G (cp), H	S	2·56	13·37	15·93	0·161	G
94	17	—	G (cp), H	U	3·64	10·40	14·04	0·259	G
95	94	no	G (cp), H	S	5·00	38·57	43·57	0·115	G
96	18	—	G (cp), H	U	4·13	15·36	19·49	0·212	G
97	93	no	G (cp), H	S	6·94	84·70	91·64	0·076	G
98	18	—	G (cp), H	U	4·88	25·52	30·40	0·161	G
99	59	no	A (cp), H	S	3·91	10·13	14·04	0·279	G
100	17	—	A (cp), H	U	3·39	5·25	8·64	0·392	G
101	24	no	A (cp), H	S	2·72	1·18	3·90	0·696	G
119	65	—	G (L), H	U	2·56	1·77	4·33	0·592	G
126	36	no	G (L), H	S	2·89	1·43	4·32	0·670	G
127	45	—	G (L), H	U	2·32	0·42	2·74	0·846	G
128	40	no	G (L), H	S	8·04	125·85	133·89	0·060	G
134	46	—	G (L), H	U	6·26	359·97	366·23	0·017	H
135	42	—	G (cp), H	U	6·30	360·34	366·64	0·017	H, G

136 . .	48	—	G (L), H	U	6·26	360·51	366·77	0·017	H
137 . .	38	no	G (L), H	S	5·56	360·43	365·99	0·015	H, G
138 . .	53	—	A (W), H	U	4·90	360·47	365·37	0·013	H
139 . .	38	no	G (L), H	S	8·10	354·99	363·08	0·022	H
140 . .	49	—	G (L), H	U	0·71	361·63	362·34	0·002	H
151 . .	47	—	H	U	0	362·01	362·01	0·000	H
152 . .	22	no	H	S	0	362·18	362·18	0·000	H
159 . .	26	no	G (L), H	S	6·21	53·69	59·90	0·104	G
160 . .	33	no	G (L), H	S	6·48	59·71	66·19	0·098	G
167 . .	44	no	G (L), H	S	7·84	70·31	78·15	0·100	G
176 . .	41	—	G (B), H	U	2·75	1·91	4·66	0·591	G
177 . .	41	G	G (B), H	S	2·72	0·62	3·34	0·814	G
185 . .	104	—	G (B), H	U	7·96	182·84	190·80	0·042	G
186 . .	92	no	G (B), H	S	7·06	362·58	369·64	0·019	G, H
188 . .	128	A	G (B), H	S	6·81	58·29	65·10	0·105	G
189 . .	128	A	G (B), H	S	7·82	144·85	152·67	0·051	G
190 . .	104	—	G (B), H	U	7·38	101·93	109·31	0·068	G
214 . .	134	A	G (B), H	S	6·58	347·37	353·95	0·019	G
215 . .	118	A	G (B), H	S	8·18	238·89	247·07	0·033	G
218 . .	121	—	A (B), H	U	6·96	91·63	98·59	0·071	A, G (?)
219 . .	86	—	A (B), H	U	7·66	102·51	110·17	0·070	G
220 . .	67	A	A (B), H	S	5·29	32·65	37·94	0·139	G
221 . .	110	A	A (B), H	S	5·86	91·60	97·46	0·060	G
228 . .	50	A+G	G (B), H	S	2·63	1·01	3·64	0·722	G
229 . .	50	G+A	G (B), H	S	2·37	0·16	2·53	0·937	G
235 . .	121	G+A	G (B), H	S	6·15	41·78	47·93	0·128	G
236 . .	120	—	A (B), H	U	7·17	103·42	110·59	0·065	A

* A, anhydrite; G, gypsum; H, halite. (W), from Wathlingen; (B) from Billingham; (L), from Lockport; (cp), Baker reagent grade material.

† S, from supersaturation or excess H₂O side by precipitation; U, from undersaturation or excess solid side.

‡ A, anhydrite; G, gypsum; H, halite.

TABLE 9

Experimental data on the system CaSO$_4$–NaCl–H$_2$O. II. 50° C Isotherm at 1 atm pressure

Run no.	Length, days	Seeds	Starting material*	Approach†	CaSO$_4$	NaCl	(CaSO$_4$+NaCl)	$\dfrac{\text{CaSO}_4}{(\text{CaSO}_4+\text{NaCl})}$	Solid phases‡
							Solution results, g/kg H$_2$O where applies		
10	19	no	A (cp), H	S	5·46	35·96	41·42	0·132	G
12	11	—	A (cp), H	U	2·53	3·00	5·53	0·457	A§
13	11	—	A (cp), H	U	3·09	6·68	9·77	0·323	G
14	14	no	A (cp), H	S	2·65	0	2·65	1·000	G
15	7	—	A (cp), H	U	2·94	8·47	11·41	0·257	G
16	29	no	A (cp), H	S	5·53	37·30	42·83	0·129	G
19	7	—	G (L)	U	2·19	0	2·19	1·000	G
20	8	—	G (cp)	U	2·25	0	2·25	1·000	G
21	2	—	A (W)	U	1·73	0	1·73	1·000	A§
22	3	A	G (cp)	S	2·67	0	2·67	1·000	G
23	4	—	A (W)	U	1·61	0	1·61	1·000	A§
24	1	—	A (W)	U	1·34	0	1·34	1·000	A§
25	14	A	A (W), H	S	5·77	37·01	42·78	0·135	G
27	14	—	A (W), H	U	2·29	3·45	5·74	0·399	A§
34	26	—	A (W), H	U	2·62	1·06	3·68	0·712	G
39	48	A	A (W), H	S	7·35	82·59	89·94	0·087	G
40	15	A	A (W), H	S	4·82	20·51	25·33	0·190	G
41	16	—	A (W), H	U	3·38	12·48	15·86	0·216	A§
42	35	A	A (W)	S	3·24	0	3·24	1·000	G
44	15	—	A (W), H	U	2·19	0·38	2·57	0·852	A§
48	28	—	A (W), H	U	3·12	328·39	331·51	0·009	A§, G(?)
49	48	no	A (cp), H	S	5·41	359·93	365·34	0·015	H
50	60	—	G (cp), H	U	4·45	360·90	365·35	0·012	H
51	53	no	G (cp), H	S	5·94	360·40	366·34	0·016	H
52	61	—	A (W), H	U	0·69	363·04	363·73	0·002	H
54	38	—	G (L), H	U	5·12	360·71	365·83	0·014	H
55	52	no	G (L), H	S	6·38	366·23	372·61	0·017	H
63	48	—	G (L), H	U	6·68	298·70	305·38	0·022	G, H
64	64	no	G (L), H	S	6·35	365·62	371·97	0·017	H, G
68	36	no	A (cp), H	S	1·42	366·47	367·90	0·004	H
69	36	—	H	U	0	363·70	363·70	0·000	H

70 . .	52	no	H	S	0	365·00	365·00	0·000	H
77 . .	33	—	A (W), H	U	2·52	1·77	4·29	0·589	G
103 . .	16	—	A (W)	U	2·05	0	2·05	1·000	A§
104 . .	28	—	A (W)	U	2·17	0	2·17	1·000	G
105A . .	59	no	A (W), H	S	2·41	1·08	3·49	0·690	G
107A . .	66	no	A (W), H	S	8·11	150·48	158·59	0·051	G
108A . .	50	—	A (W), H	U	5·55	90·56	96·11	0·053	A§
109 . .	50	—	A (W), H	U	1·74	0·41	2·15	0·809	A§
110 . .	73	A	A (W), H	S	2·50	0·59	3·09	0·808	G
111 . .	52	—	A (W), H	U	4·65	37·09	41·74	0·111	G
113 . .	53	—	A (W), H	U	5·79	64·95	70·74	0·082	A§
114 . .	55	—	A (W), H	U	2·07	2·70	4·77	0·434	A§
153 . .	24	no	G (cp), H	S	3·76	4·12	7·88	0·477	G
154 . .	20	A	A (B), H	S	3·07	4·73	7·80	0·394	G
155 . .	10	no	G (cp), H	S	2·82	2·70	5·52	0·510	G
156 . .	33	—	A (B), H	U	2·65	2·04	4·69	0·565	G
168 . .	34	—	A (B), H	U	2·51	3·25	5·76	0·436	A§
169 . .	34	—	G (L), H	U	2·74	2·87	5·61	0·488	G
170 . .	26	A	A (B), H	S	3·10	5·93	9·03	0·343	G
171 . .	35	—	A (B), H	U	5·94	67·31	73·25	0·081	A§
174 . .	20	A	A (B), H	S	2·60	0·45	3·05	0·852	G
175 . .	36	—	A (B), H	U	1·73	0·44	2·17	0·797	A§
191 . .	30	A	A (B), H	S	6·75	364·27	371·02	0·018	G
192 . .	44	—	A (B), H	U	5·05	316·77	321·82	0·016	A§
193 . .	50	—	A (B), H	U	4·08	108·80	112·88	0·036	G
194 . .	79	—	G (B), H	U	7·41	104·14	111·55	0·066	G
196 . .	21	—	A (B), H	U	5·91	60·78	66·69	0·089	G
200 . .	28	no	A (B), H	S	6·56	65·34	71·90	0·091	G
203 . .	14	no	A (B), H	S	7·77	241·11	248·88	0·031	G
204 . .	56	—	G (B), H	U	6·27	58·49	64·76	0·097	G
205 . .	56	—	A (B), H	U	4·11	24·85	28·96	0·142	A§
206 . .	56	—	A (B), H	U	5·97	99·54	105·51	0·057	A§
207 . .	47	A	A (B), H	S	3·09	5·18	8·27	0·374	G
208 . .	46	A	A (B), H	S	2·33	0·98	3·31	0·704	G
213 . .	56	—	G (B), H	U	2·22	0·48	2·70	0·824	G
216 . .	52	—	A (B), H	U	1·77	·0·34	2·11	0·840	A§
217 . .	30	A	A (B), H	S	2·24	0·64	2·88	0·778	G

* A, anhydrite; G, gypsum; H, halite. (W), from Wathlingen; (B), from Billingham; (L), from Lockport; (cp), Baker reagent grade material.
† S, from supersaturation or excess H₂O side by precipitation; U, from under-saturation or excess solid side.
‡ A, anhydrite; G, gypsum; H, halite. § Detrital.

TABLE 10

Experimental data on the system $CaSO_4$–$NaCl$–H_2O. III. $70°$ C Isotherm at 1 atm pressure

Run no.	Length, days	Seeds	Starting material*	Approach†	Solution results, g/kg H_2O where applies				Solid phases‡
					$CaSO_4$	NaCl	$(CaSO_4 + NaCl)$	$\dfrac{CaSO_4}{(CaSO_4 + NaCl)}$	
7‖ . .	4	no	A (cp), H	S	5·01	12·33	17·34	0·289	G
8‖ . .	4	A	A (cp), H	S	2·46	6·31	8·77	0·281	G
61 . .	10	no	A (cp)	S	2·14	0	2·14	1·000	G
65 . .	9	A	G (cp)	S	2·25	0	2·25	1·000	G
71 . .	12	A	A (cp), H	S	2·94	4·64	7·58	0·388	G
73 . .	11	A	G (L)	S	2·01	0	2·01	1·000	G
74 . .	25	—	G (L)	U	2·05	0	2·05	1·000	G
75 . .	26	—	A (W)	U	2·25	0	2·25	1·000	G
78 . .	21	A	A (cp), H	S	5·30	34·35	39·65	0·134	G
79 . .	9	A	A (cp), H	S	6·56	59·47	66·03	0·099	G
80 . .	9	A	A (cp), H	S	2·62	25·63	28·25	0·093	G
86 . .	15	no	A (cp), H	S	4·02	16·57	20·59	0·195	G
87 . .	10	no	A (cp), H	S	4·96	30·14	35·10	0·141	G
88 . .	16	no	A (cp), H	S	6·4	90·0	96·4	0·066	G
91 . .	15	—	A (cp), H	U	3·84	12·83	16·67	0·231	G
92 . .	11	—	A (cp), H	U	3·94	14·83	18·77	0·210	G
93 . .	13	—	A (cp), H	U	3·94	17·97	21·92	0·189	G
105 . .	15	—	A (cp), H	U	4·22	28·79	32·99	0·127	G
106 . .	10	no	A (cp), H	S	7·52	112·12	119·63	0·063	G
107 . .	12	—	A (cp), H	U	2·63	2·76	5·39	0·488	G
108 . .	12	—	A (cp), H	U	2·36	1·19	3·56	0·665	G
116 . .	58	—	A (B), H	U	3·09	2·17	5·26	0·587	G
117 . .	45	—	A (B), H	U	2·20	0·77	2·97	0·740	G
121 . .	33	—	A (B), H	U	4·87	28·88	33·75	0·144	G
122 . .	14	no	A (B), H	S	5·08	32·95	38·03	0·134	G
124 . .	17	no	A (B), H	S	6·56	67·54	74·10	0·089	G
129 . .	17	A	A (B)	S	2·00	0	0	1·000	G
130 . .	17	—	A (B), H	U	3·72	375·07	379·79	0·010	H
131 . .	17	—	A (B), H	U	3·35	374·34	377·69	0·009	G
132 . .	19	—	G (L), H	U	6·36	373·69	380·05	0·017	B, H

No.										
133	.	.	19	—	A (B), H	U	1·41	0·47	1·88	0·750	A§
142	.	.	19	—	A (B), H	U	3·80	374·21	378·01	0·010	H
143	.	.	19	—	G (L), H	U	5·84	374·14	379·98	0·015	H, B
144	.	.	10	no	A (B), H	S	6·82	373·71	380·53	0·017	H, B
146	.	.	28	—	A (B), H	U	1·50	336·94	338·44	0·004	H
147	.	.	28	—	G (L), H	U	6·21	375·61	381·82	0·016	H, B
148	.	.	19	no	A (B), H	S	6·97	373·80	380·77	0·018	H, B (?)
149	.	.	28	—	A (B), H	U	4·45	357·35	361·80	0·012	A§
150	.	.	29	—	G (L), H	U	6·27	335·69	341·96	0·018	B
157	.	.	20	—	A (B), H	U	1·54	1·15	2·69	0·573	A§
158	.	.	14	no	A (B), H	S	7·26	371·11	378·37	0·019	H, G, B
162	.	.	33	—	A (B), H	U	4·23	335·03	339·26	0·013	A§
163	.	.	35	—	G (L), H	U	8·05	147·28	155·33	0·052	G
164	.	.	28	no	A (B), H	S	0·98	375·67	376·65	0·003	H
165	.	.	21	—	A (B), H	U	0·95	374·89	375·84	0·003	H
166	.	.	22	no	A (B), H	S	5·29	33·72	39·01	0·136	G
172	.	.	15	A	A (B)	S	2·27	0	2·27	1·000	G
173	.	.	21	—	A (B), H	U	1·34	0·82	2·16	0·620	A§
178	.	.	13	A	A (B), H	S	6·92	372·27	379·19	0·018	B
179	.	.	16	A	A (B), H	S	8·42	278·37	286·79	0·029	B, G
180	.	.	40	—	A (B), H	U	3·57	7·89	11·46	0·312	G
181	.	.	39	A	A (B), H	S	4·61	21·42	26·03	0·177	G
182	.	.	33	A	A (B), H	S	7·03	347·98	355·01	0·020	B, H (?)
183	.	.	40	—	A (B), H	U	5·64	375·37	381·01	0·015	G, H
197	.	.	50	—	A (B), H	U	4·23	18·24	22·47	0·188	G
198	.	.	44	A	A (B), H	S	4·61	21·60	26·21	0·176	G.
199	.	.	43	—	A (B), H	U	3·66	8·34	12·00	0·305	G.
201	.	.	50	A	A (B), H	S	2·28	0·69	2·97	0·767	G.
202	.	.	43	—	A (B), H	U	6·98	120·22	127·20	0·055	G
209	.	.	47	A	A (B), H	S	2·48	1·44	3·92	0·632	G
210	.	.	48	—	A (B), H	U	2·06	0·67	2·73	0·753	G
211	.	.	49	A	A (B), H	S	2·19	1·10	3·29	0·666	G
212	.	.	52	A	A (B), H	S	2·12	0·38	2·50	0·850	G

* A, anhydrite; G, gypsum; H, halite. (W), from Wathlingen; (B), from Billing-
ham; (L), from Lockport; (cp), Baker reagent grade material.

† S, from supersaturation or excess H₂O side by precipitation; U, from under-
saturation or excess solid side.

‡ A, anhydrite; G, gypsum; B, bassanite; H, halite.

§ Detrital.

‖ 74° C.

pressure effect on the transition temperature, $dP/dT = \Delta S/\Delta V$, within the binary system, should also be modified, in light of this revision and in light of more recent data on the molar volumes of gypsum and of anhydrite.

We take

$$\Delta S\ (T, P = 1\ \text{atm}) = -148{\cdot}42 - 0{\cdot}052\ T + 30{\cdot}98\ \ln T \pm 0{\cdot}86\ \text{e.u.}$$

which is obtained by differentiating equation (3). We also take $V^G = 74{\cdot}31 \pm 0{\cdot}16$ cc and $V^A = 45{\cdot}94 \pm 0{\cdot}05$ cc, both per mole $CaSO_4$, at room temperature (R. A. Robie & P. M. Bethke, 1962, written communication), and $V^{\text{water}} = 18{\cdot}20$ cc/mole at 46° C. Ignoring the volume difference between room temperature and 46° for the solids, we have, assuming $P_{\text{total}} = P_{\text{water}}$, $dP/dT = 70 \pm 1{\cdot}9$ atm/deg. The transition temperature, T_t, is 53° C at 500 atm. For comparison, the value of T_t at 500 bars is given by MacDonald (1953, p. 887) at 46°; that of dP/dT is given as 85·4 bar/deg.

If the solids were under lithostatic pressure but the liquid were under hydrostatic pressure (Thompson, 1955; MacDonald, 1953), calculation gives
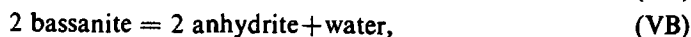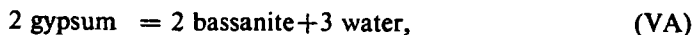
$$dP_{\text{total}}/dT = -42{\cdot}6 \pm 0{\cdot}7\ \text{atm/deg,}$$

with $T_t = 34°$ at 500 atm. MacDonald's figures (1953, p. 888) are −39·45 bar/deg and T_t (500 bars) = 27° C.

APPENDIX V

BASSANITE IN NATURE

Bassanite has been reported from a number of natural environments. Palache, Berman, & Frondel (1951, p. 476) quote its occurrence in cavities of volcanic ejecta from Vesuvius. Bundy (1956, p. 249) and Goodman (1957, p. 111) found this mineral in evaporite sequences associated with gypsum and anhydrite, in Indiana and in Nova Scotia, respectively. Palmer (1957, p. 241), Allen & Kramer (1953) and Smith & Pratt (1957, p. 52) report this mineral in various parts of the Mojave desert in California; Popov and Voreb'ev (1947) report it from similar deposits in central Asia. Goodman (1957, p. 112) reported that the Nova Scotia bassanite, found in drill cores, replaced both gypsum and anhydrite, and therefore presumably was not an alteration product caused by the drilling process.

On the basis of numerous experimental works (see Posnjak, 1938, p. 268) and the thermochemical data of Kelley *et al.* (1941), bassanite is unstable relative to gypsum and anhydrite at one atmosphere pressure under any temperature and salinity conditions. In order to see whether bassanite could be stabilized by pressure, either relative to gypsum or relative to anhydrite, calculations analogous to those of MacDonald were made. The calculations pertain to two limiting conditions: (1) $P_{\text{total}} = P_{\text{water}}$; (2) $P_{\text{water}}/P_{\text{total}} = \rho_{\text{water}}/\rho_{\text{rock}}$. The molar entropy of bassanite, $\approx 31{\cdot}8$ e.u., is given in Table 6; the molar volume, 50·4 cc per formula $CaSO_4$, is computed from the cell data of Donnay & Nowacki (1954, p. 407).[1] The reactions are

2 gypsum	= 2 bassanite + 3 water,	(VA)
2 bassanite	= 2 anhydrite + water,	(VB)
and 4 bassanite	= 3 anhydrite + gypsum.	(VC)

[1] The cell-dimension data agree closely with those given by Flörke (1952, p. 194). The 'calculated density' of Donnay & Nowacki, however, disagrees with their own cell-dimension data.
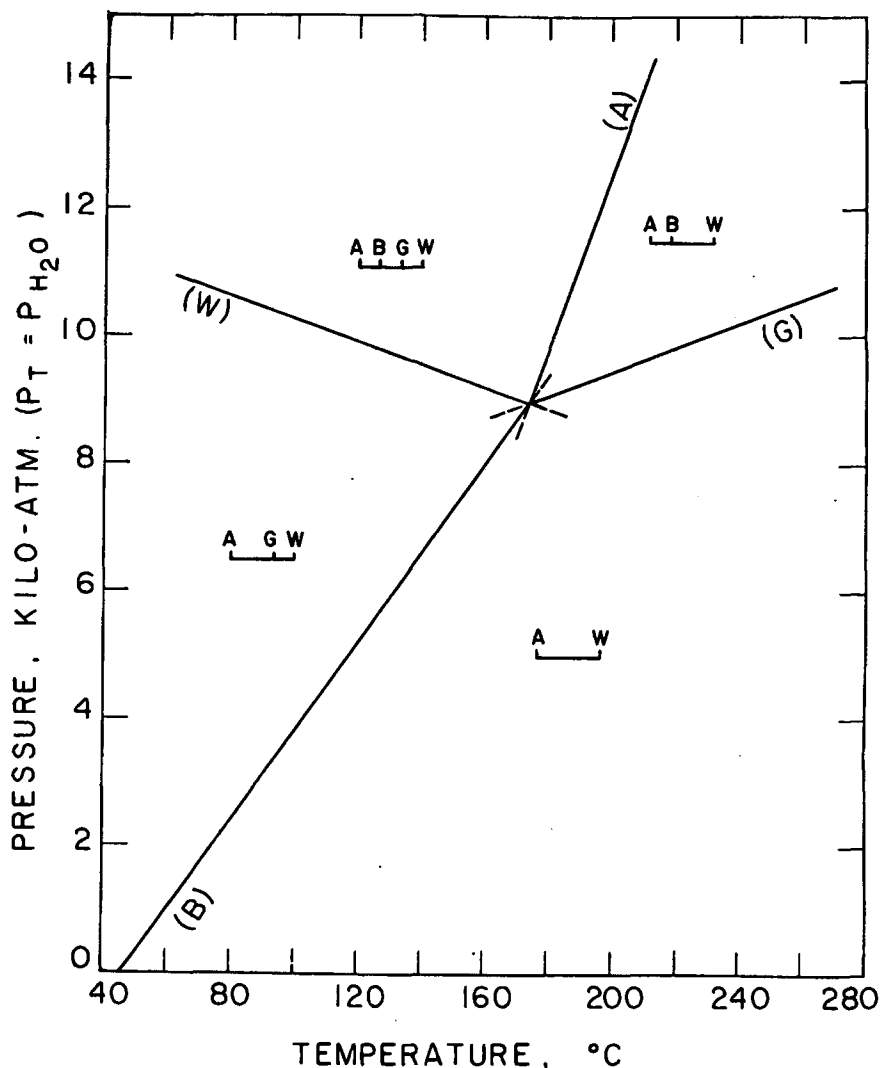
FIG. 14. The quadruple point gypsum (G, $CaSO_4.2H_2O$)—anhydrite (A, $CaSO_4$)—bassanite (B, $CaSO_4.\frac{1}{2}H_2O$)—solution (W) in the binary system $CaSO_4$–H_2O. Data used in the calculations of the slopes are given in the text. Letters in parenthesis indicate the phases not participating in the univariant equilibria. Location of the quadruple point was determined by the intersection of curve (B) and curve (G). For curve (B), the 'consistent' data are used; for curve (G), the data of Kelley *et al.* were used. All univariant lines are assumed to be rectilinear.

ΔS for (VA) is ≈ 21 e.u., ΔS for reaction (VB) is ≈ 4.2 e.u., and ΔS for reaction (VC) is ≈ -4.3 e.u. Therefore, the initial slopes are given by

$$(dP/dT)_{P_{total}=P_{water}} = 138 \text{ atm/deg}$$

and $\qquad (dP/dT)_{P_{total}/P_{water}=\rho_{rock}/\rho_{water}} = -35 \text{ atm/deg}$

for reaction (VA), $\qquad (dP/dT)_{P_{total}=P_{water}} = 19 \text{ atm/deg}$

and $\qquad (dP/dT)_{P_{total}/P_{water}=\rho_{rock}/\rho_{water}} = -5 \text{ atm/deg}$

for reaction (VB), and $\qquad (dP/dT) = -17 \text{ atm/deg}$

6233.1 $\qquad\qquad\qquad\qquad\qquad$ M

for reaction (VC) independent of the nature of the pressure medium because only solid phases are involved. The slopes for the reaction between gypsum and anhydrite, as previously stated, are $+70.0$ atm/deg and -42.3 atm/deg for the two limiting cases, respectively.

Using these data and assuming $P_T = P_{H_2O}$, it is possible to construct a quadruple point involving the three solid phases and water in the binary system $CaSO_4$–H_2O. This construction assumes constant values for the slopes of the univariant curves; obedience of the Morey–Schreinemakers Rule is a necessary condition for the quadruple point to be a stable one (see Morey & Williamson, 1918). The only internally consistent construction is the one given in Fig. 14; the notation is that used, for instance, by Niggli (1954, p. 374). It appears that bassanite might be stable under high pressure in abnormally cold spots in the crust, though the requisite pressure hardly explains the petrographical observations. On the other hand, the occurrence of bassanite in industrial and experimental works clearly shows the possibility of its metastable formation under wide ranges of conditions. This phase is unlikely to be precipitated directly from sea water owing to the high temperature required for even its metastable formation; however, upon deep burial the transformation from gypsum or anhydrite into bassanite should be possible.

REFERENCES

ADAMS, J. E., 1944. Upper Permian Ochoa series of Delaware Basin, West Texas and southeastern New Mexico. *Amer. Assoc. petrol. Geol. Bull.* 28, 1596–1625.

ALLEN, R. D., & KRAMER, H., 1953. Occurrence of bassanite in two desert basins in southeastern California. *Amer. Min.* 38, 1266–8.

BLOUNT, C. W., & DICKSON, F. W., 1962. Solubility of anhydrite in aqueous NaCl solutions at elevated temperatures and pressures [abstract]. *Geol. Soc. America Special Paper*, 68, 8–9.

BOCK, E., 1961. On the solubility of anhydrous calcium sulphate and of gypsum in concentrated solutions of sodium chloride at 25° C, 30° C, 40° C, and 50° C. *Canadian J. Chem.* 39, 1746–51.

BORCHERT, H., 1959. *Ozeane Salzlagerstätten*. Berlin, Gebrüder Borntraeger. 237 pp.

—— & BAIER, E., 1953. Zur Metamorphose ozeaner Gipsablagerungen. *Neues Jb. Mineral. Abh.* 86, 103–54.

BRAITSCH, O., 1962a. *Entstehung und Stoffbestand der Salzlagerstätten*. Berlin, Springer Verlag. 232 pp.

—— 1962b. Die Entstehung der Schichtung in rhythmisch geschichteten Evaporiten. *Geol. Rundschau*, 52, 405–17.

BRANNOCK, W. W., & SHAPIRO, L., 1962. Rapid analysis of silicate, carbonate, and phosphate rocks. *U.S. Geol. Survey Bull.* 1144-A. 56 pp.

✱ BRIGGS, L. I., 1958. Evaporite facies. *J. sed. Petrology*, 28, 46–56.

BUNDY, W. M., 1956. Petrology of gypsum-anhydrite deposits in southwestern Indiana. Ibid. 26, 240–52.

CAMERON, F. K., 1901. Solubility of gypsum in aqueous solutions of sodium chloride. *J. phys. Chem.* 5, 556–76.

CONLEY, R. F., & BUNDY, W. M., 1958. Mechanism of gypsification. *Geochem. et Cosmoch. Acta*, 15, 57–72.

D'ANS, J., BREDTSCHNEIDER, D., EICK, H., & FREUND, H. E., 1955. Untersuchungen über die Calciumsulfate. *Kali und Steinsalz* (Ser. 1), Heft 9, 17–38.

—— & KÜHN, R., 1960. Bemerkungen zur Bildung und zu Umbildungen ozeanischer Salzlagerstätten. *Kali und Steinsalz*, Heft 3, 69–84.

DEER, W. A., HOWIE, R. A., & ZUSSMAN, J., 1962. *Rock-forming minerals*. Vol. 5. New York, John Wiley and Sons. 371 pp.

DELLWIG, L. F., 1955. Origin of the salina salt of Michigan. *J. sed. Petrology*, 25, 83–110.

DICKSON, F. W., BLOUNT, C. W., & TUNNEL, G., 1963. Use of hydrothermal solution equipment to determine the solubility of anhydrite in water from 100° C to 275° C and from 1 bar to 1000 bars pressure. *Amer. J. Sci.* **261**, 61–78.

DONNAY, J. D. H., & NOWACKI, W., 1954. Crystal data. *Geol. Soc. America Mem.* **60**, 719 pp.

FLÖRKE, O. W., 1952. Kristallographische und röntgenometrische Untersuchungen im System CaSO₄–CaSO₄ . 2H₂O. *Neues Jb. Mineral. Abh.* **84**, 189–240.

GIAUQUE, W. F., & STOUT, J. W., 1936. The entropy of water and the Third Law of Thermodynamics. The heat capacity of ice from 15° to 273° K. *Amer. chem. Soc. J.* **58,** 1144–50.

GOODMAN, N. R., 1957. Gypsum in Nova Scotia and its associated minerals. *In* The geology of Canadian industrial mineral deposits. *Canadian Inst. Mining Metallurgy, Indus. Minerals Div.* 110–14.

HALL, R. E., ROBB, J. A., & COLEMAN, C. E., 1926. The solubility of calcium sulfate at boiler-water temperatures. *Amer. chem. Soc. J.* **48**, 927–38.

HILL, A. E., 1937. The transition temperature of gypsum to anhydrite. Ibid. **59**, 2242–4.

International Critical Tables, 1926–1933. New York, McGraw-Hill Book Co.

KELLEY, K. K., 1960. Contributions to the data on theoretical metallurgy, XIII. High-temperature heat-content, heat-capacity, and entropy data for the elements and inorganic compounds. *U.S. Bur. Mines Bull.* **584.** 232 pp.

—— SOUTHARD, J. C., & ANDERSON, C. T., 1941. Thermodynamic properties of gypsum and its dehydration products. *U.S. Bur. Mines Tech. Paper,* **625.** 73 pp.

KLOTZ, I. M., 1950. *Chemical thermodynamics.* New York, Prentice-Hall, Inc. 369 pp.

LAVOISIER, A. L., 1768. *Analyse du gypse: Mémoires de mathématique et de physique, présentés a l'Académie royale des sciences, par divers savans, et lus dans ses assemblées,* **5**, 341–57.

MACDONALD, G. J. F., 1953. Anhydrite–gypsum equilibrium relations. *Amer. J. Sci.* **251**, 884–98.

MADGIN, W. M., & SWALES, D. A., 1956. Solubilities in the system CaSO₄–NaCl–H₂O at 25° and 35°. *J. appl. Chem.* **6**, 482–7.

MARSAL, D., 1952. Der Einfluss des Druckes auf das System CaSO₄–H₂O. *Heidelb. Beitr. Mineral. Petrog.* **3**, 289–96.

MOREY, G. W., & WILLIAMSON, E. D., 1918. Pressure-temperature curves in univariant systems. *Amer. chem. Soc. J.* **40**, 59–84.

NIGGLI, P., 1954. *Rocks and mineral deposits* (R. L. Parker, translator). San Francisco, W. H. Freeman and Co. 559 pp.

PALACHE, C., BERMAN, H., & FRONDEL, C., 1951. *Dana's system of mineralogy.* Vol. 2. New York, John Wiley and Sons. 1124 pp.

PALMER, A. R., 1957. Miocene arthropods from the Mojave Desert, California. *U.S. Geol. Survey Prof. Paper* **294-G**, 237–80.

PARTRIDGE, E. P., & WHITE, A. H., 1929. The solubility of calcium sulfate from 0° to 200°. *Amer. chem. Soc. J.* **51**, 360–70.

POPOV, V. I., & VOREB'EV, A. L., 1947. Hemihydrate in the desert deposits of Middle Asia. *Zapiski Vserossii mineral. obshchestva,* ser. 2, **76**, 268–70 (Chem. Abst. **43**, 2897 h, 1949).

POSNJAK, E., 1938. The system CaSO₄–H₂O. *Amer. J. Sci.,* 5th ser., **35A**, 247–72.

—— 1940. Deposition of calcium sulfate from sea water. Ibid. **238**, 559–68.

PRIGOGINE, I., & DEFAY, R., 1954. *Chemical thermodynamics.* London, Longmans Green and Co. 543 pp.

RAYMOND, L. R., 1952. Some geological results from the exploration for potash in north-east Yorkshire. *Geol. Soc. London Quart. J.* **108**, 283–310.

ROBINSON, R. A., & STOKES, R. H., 1955. *Electrolyte solutions.* London, Butterworths Scientific Publications. 512 pp.

ROEDDER, E., 1963. Studies of fluid inclusions, II: Freezing data and their interpretation. *Econ. Geol.* **58**, 167–211.

ROSSINI, F. D., WAGMAN, D. D., EVANS, W. H., LEVINE, S., & JAFFE, I., 1952. Selected values of chemical thermodynamic properties. *U.S. Bur. Standards Circ.* **500.** 1268 pp.

SCHALLER, W. T., & HENDERSON, E. P., 1932. Mineralogy of drill cores from the potash field of New Mexico and Texas. *U.S. Geol. Survey Bull.* **833.** 124 pp.

SCRUTON, P. C., 1953. Deposition of evaporites. *Amer. Assoc. petroleum Geologists Bull.* **37**, 2498–512.

SHTERNINA, E. B., 1947. Rastvorimost gipsa v vodnykh rastovarakh soley. *Akad. nauk S.S.S.R., Izvestiya sektora fiziko-khimicheskogo analiza,* **17**, p. 351–69. (English translation, Solubility of gypsum in aqueous solutions of salts, by A. J. Shneiderov, *Intern. Geology Rev.* **2**, 605–16, 1960.)

—— 1957. O maksimume na izotermakh rastvorimosti sul'fata i karbonata kal'tsiya. *Zhur. neorgan. khimii,* **2**, 933–7. (English translation, On the maximum of the solubility isotherms of calcium sulfate and carbonate. *J. inorgan. Chem. USSR,* **2**, 344–51.)

SMITH, G. I., & PRATT, W. P., 1957. Core logs from Owens, China, Searles, and Panamint Basins, California. *U.S. Geol. Survey Bull.* **1045-A.** 62 pp.

STEWART, F. H., 1953. Early gypsum in the Permian evaporites of northeastern England. *Proc. Geol. Assoc.* **64**, 33–39.

—— 1963. Marine evaporites, Chap. Y *in* Fleischer, M., ed., *Data of Geochemistry*, Sixth edition. *U.S. Geol. Survey Prof. Paper*, **440**-Y. 52 pp.

THOMPSON, J. B., Jr., 1955. The thermodynamic basis for the mineral facies concept. *Amer. J. Sci.* **253**, 65–103.

TORIUMI, T., & HARA, R., 1934. On the transition of calcium sulfate in water and in concentrated sea water. *Chem. Soc. Japan J.* **55**, 1051–9 (in Japanese).

—— KUWAHARA, T., & HARA, R., 1938. On the calcium sulphate in sea water, II. Solubilities of calcium sulphate hemihydrate in sea water of various concentrations at 65°–150° C. *Sendai, Tôhoku Imperial University Technology Rept.* **12**, 560–71.

UDDEN, J. A., 1924. Laminated anhydrite in Texas. *Geol. Soc. America Bull.* **35**, 347–54.

VAN'T HOFF, J. H., 1912. *Untersuchungen über die Bildungsverhältnisse der ozeanischen Salzablagerungen, insbesondere des Stassfurter Salzlagers.* Leipzig, H. Precht und E. Cohen. 374 pp.

WEISER, H. B., MILLIGAN, W. O., & EKHOLM, W. C., 1936. The mechanism of the dehydration of calcium sulfate hemihydrate. *Amer. chem. Soc. J.* **58**, 1261–5.

ZEN, E-AN, 1959. Early stages of evaporite deposition [abstract]. *Geol. Soc. America Bull.* **70**, 1704.

—— 1960. Early stages of evaporite deposition. *U.S. Geol. Survey Prof. Paper*, **400**-B, B458–B461.

—— 1962. Phase equilibrium studies of the system $CaSO_4$–$NaCl$–H_2O at low temperatures and 1 atmosphere pressure [abstract]. *Geol. Soc. America Special Paper*, **68**, 306.

—— 1963. Components, phases, and criteria of chemical equilibrium in rocks. *Amer. J. Sci.* **261**, 929–42.